Biochimica et Biophysica Acta 1838 (2014) 287–299

Contents lists available at ScienceDirect

Biochimica et Biophysica Acta

journal homepage: www.elsevier.com/locate/bbamem

Rubber particle proteins, HbREF and HbSRPP, show different interactions with model membranes☆

Karine Berthelot [a,b,*], Sophie Lecomte [c,d], Yannick Estevez [a,b], Vanessa Zhendre [e,f], Sarah Henry [c,d,g], Julie Thévenot [a,b], Erick J. Dufourc [c,d,e,f], Isabel D. Alves [c,d], Frédéric Peruch [a,b,*]

[a] CNRS, LCPO, UMR 5629, F-33600 Pessac, France
[b] Univ. Bordeaux, LCPO, UMR 5629, F-33600 Pessac, France
[c] CNRS, CBMN, UMR 5248, F-33600 Pessac, France
[d] Univ. Bordeaux, CBMN, UMR 5248, F-33600 Pessac, France
[e] CNRS, IECB, UMS 3033, F-33600 Pessac, France
[f] Univ. Bordeaux, IECB, UMS 3033, F-33600 Pessac, France
[g] CNRS, IBGC, UMR 5095, F-33000 Bordeaux, France

ARTICLE INFO

Article history:
Received 24 May 2013
Received in revised form 27 August 2013
Accepted 31 August 2013
Available online 12 September 2013

Keywords:
REF
SRPP
Hevea brasiliensis latex
Natural rubber
Amyloid
Plant membrane

ABSTRACT

The biomembrane surrounding rubber particles from the hevea latex is well known for its content of numerous allergen proteins. HbREF (Hevb1) and HbSRPP (Hevb3) are major components, linked on rubber particles, and they have been shown to be involved in rubber synthesis or quality (mass regulation), but their exact function is still to be determined. In this study we highlighted the different modes of interactions of both recombinant proteins with various membrane models (lipid monolayers, liposomes or supported bilayers, and multilamellar vesicles) to mimic the latex particle membrane. We combined various biophysical methods (polarization-modulation-infrared reflection-adsorption spectroscopy (PM-IRRAS)/ellipsometry, attenuated-total reflectance Fourier-transform infrared (ATR-FTIR), solid-state nuclear magnetic resonance (NMR), plasmon waveguide resonance (PWR), fluorescence spectroscopy) to elucidate their interactions. Small rubber particle protein (SRPP) shows less affinity than rubber elongation factor (REF) for the membranes but displays a kind of "covering" effect on the lipid headgroups without disturbing the membrane integrity. Its structure is conserved in the presence of lipids. Contrarily, REF demonstrates higher membrane affinity with changes in its aggregation properties, the amyloid nature of REF, which we previously reported, is not favored in the presence of lipids. REF binds and inserts into membranes. The membrane integrity is highly perturbed, and we suspect that REF is even able to remove lipids from the membrane leading to the formation of mixed micelles. These two homologous proteins show affinity to all membrane models tested but neatly differ in their interacting features. This could imply differential roles on the surface of rubber particles.

© 2013 Elsevier B.V. All rights reserved.

1. Introduction

Hevea brasiliensis (Willd. Ex A. Juss) Muëll. Arg is the main worldwide resource of latex and natural rubber (NR), which is a biopolymer of high economic interest mainly composed of *cis*-1,4-polyisoprene. Latex is indeed produced by laticifers after tapping and is a white cytoplasmic colloidal suspension containing mainly rubber particles but also non-rubber particles, organelles, proteins and serum [1]. Hevea latex has a bimodal particle size distribution [2,3], containing spherical particles [4] smaller than 0.4 μM in diameter (SRP, small rubber particles) or larger than 0.4 μM (LRP, large rubber particles) [5,6]. Latex particles are negatively charged on their surface [7] and latex has a pI between 3 and 5 [8]. This confers a colloidal stability of latex at basic pH, whereas latex coagulates at low pH. A rubber particle has been described as a hydrophobic core of polyisoprene surrounded by a complex lipo-protein layer [9,10], and the particle membrane was shown to be a fluid monolayer [4,10–12]. The thickness of this layer was estimated to be around 1.5–3.0 nm [9–11]. Rubber particles contain in total about 1.6–3.7% of lipids, which are classified into neutral lipids, glycolipids and phospholipids [13–15]. Rubber lipid content and composition are clonal dependent [15] and the methods of extraction may be of particular importance [16]. The phospholipids already identified in 1930 [17] are

Abbreviations: REF, Rubber elongation factor; SRPP, Small rubber particle protein; PM-IRRAS, Polarization-modulation-infrared reflection-adsorption spectroscopy; ATR-FTIR, Attenuated-total reflectance Fourier-transform infrared; NMR, Nuclear magnetic resonance; PWR, Plasmon waveguide resonance; SUV, Small unilamellar vesicle; LUV, Large unilamellar vesicle; MLV, Multi lamellar vesicle

☆ This work highlights the possible function of SRPP-like proteins as lipid droplet-associated proteins: P.J. Horn, C.N. James, S.K. Gidda, A. Kilaru, J.M. Dyer, R.T. Mullen, J.B. Ohlrogge, K.D. Chapman KD. Identification of a new class of lipid droplet-associated proteins in plants. Plant Physiol. 162 (2013) 1926–1936.

* Corresponding authors at: Laboratoire de Chimie des Polymères Organiques, CNRS UMR 5629, ENSCBP, IPB, 16 avenue Pey-Berland, 33607 Pessac cedex, France. Tel.: +33 540002745.

E-mail addresses: kberthelot@enscbp.fr (K. Berthelot), peruch@enscbp.fr (F. Peruch).

0005-2736/$ – see front matter © 2013 Elsevier B.V. All rights reserved.
http://dx.doi.org/10.1016/j.bbamem.2013.08.025

mainly phosphatidyl choline and ethanolamine (PC and PE), but phosphatidyl inositol, serine and glycerol (PI, PS and PG) and phosphatidic acid (PA) may also be found in latex [11,15,18]. In addition, stearic (18:0), oleic (18:1) and linoleic (18:2) acids were highly represented, while smaller amounts of palmitic (16:0), palmitoleic (16:1), linolenic (18:3) and furanoid fatty acids are also present [15,18–21]. The role of phospholipids in NR branching is now highly discussed. Phospholipids could be linked at the α-terminal phosphate group of the linear polyisoprene chains, while the ω-terminal (the *trans* initiator group) could interact with proteins [22–24]. The negative charges of the lipid polar headgroups could cross-link by ionic linkages (e.g. Mg^{2+}) with the terminal phosphate or diphosphate of the polymeric chains.

Not only lipids, but also proteins, may contribute to the global negative charge of the particle surface. Recently, 186 rubber particle proteins were identified [25]. Hevea latex contains also numerous proteins and at least 14 allergens, such as Hevb3 and Hevb1 [26–30]. Hevb3 and Hevb1 are the two most abundant proteins and are also known as rubber elongation factor (HbREF) and small rubber particles protein (HbSRPP). They are acidic proteins of respectively 14.6 and 24 kDa and they both have been described as having a positive effect on rubber production [31–33]. Other homologous proteins found in *Parthenium argentatum* (Guayule Homologue of SRPP, GHS) and *Taraxacum brevicorniculatum* (TbSRPP1-5, Dandelion) have also been found having a similar effect [34,35]. They are now believed to be determinant on producing high molecular weight rubber [34,35]. Indeed, REF and SRPP have been respectively visualized by immunogold electron microscopy on the LRP and on the SRP [6,31,36–38]. TbSRPPs were also found on the dandelion rubber particle surface [35]. In addition, SRPs were described as having much higher enzymatic activity at their surface than LRPs do [5,38,39]. SRP polymer predominantly of high molecular weight, might be composed mostly of growing linear polyisoprene (with an active diphosphate group) having no free chain-end to form branch-points [40]. In contrast, LRP contains low-molecular weight rubber molecules terminated with a functional group containing fatty acid esters. Dennis and Light [31] also showed that the amount of REF protein in the whole latex was proportional to the rubber content.

In a previous study we described the structure of REF and SRPP in bulk solution and showed that if SRPP behaved like an α-helical protein, REF had amyloid and aggregative properties [41]. Aggregation could be an interesting feature taking part in latex coagulation. Preliminary results let us think that both proteins had also different behaviors in the presence of lipid monolayers. In the present work we went deeper in our observations by investigating the interactions with various membrane models (lipid monolayers, liposomes or supported bilayers and multilamellar vesicles) and by combining various biophysical methods (PM-IRRAS, ATR-FTIR, solid state NMR, PWR, fluorescence spectroscopy). We may now conclude from all our converging results that REF and SRPP exert different effects on model membranes, which could also refer to distinct functions on rubber particles.

2. Material & methods

2.1. Chemicals

Asolectin (AL), Nile red and calcein were from Sigma-Aldrich (Saint-Quentin Fallavier, France). Cardiolipins (bovine heart) and all other lipids were purchased from Avanti Polar Lipids (Alabaster, AL, USA). D_2O, $CDCl_3$, CD_3OD and deuterium-depleted water (^1H_2O) were acquired from Euriso-Top (Gif-sur-Yvette, France).

2.2. Protein purifications

The SRPP gene (GenBank accession no. AJ223388) and the REF gene (GenBank accession no. X56535) were previously constructed as codon-optimized pET24a-6His-SRPP and pET24a-6His-REF plasmids [41]. Sequences, homology and physico-chemical parameters of tagged REF and SRPP proteins are presented in Supplementary Table S1. Proteins tagged with an N-terminal 6-histidine were produced and purified as recombinant proteins following previously reported protocol [41]. For NMR experiments, proteins were freeze-dried and kept at −20 °C.

2.3. Washed rubber particles preparation

The washed rubber particles (WRPs) were purified at 4 °C from 30% non-ammoniated latex as previously described [42]. 1 mL of latex was centrifuged at 4000 *g* for 10 min, the top cream was washed with 1 mL of buffer (0.1 M Tris–HCl pH 7.4, 10 mM DTT, 5 mM $MgSO_4$), and the WRPs were then washed twice by centrifugation at 2400 *g* for 10 min and finally resuspended in buffer. Proteins on WRPs were directly denatured in loading buffer for 10 min at 100 °C, centrifuged and then run on 15% SDS-PAGE before staining with Coomassie blue.

2.4. Fluorescence confocal microscopy

Staining of WRPs with Nile red was realized by incubating the fresh WRPs with Nile red at 0.1 mg/mL in DMSO/glycerol (v/v 1:1) for 24 h at 25 °C. Incorporation of DPPE-rhodamine into the biomembrane was done by incubating the fluorescent lipids (5 μg/mL in DMSO/Glycerol) at 25 °C overnight. Confocal microscopy was realized with a Leica TCS SP5 laser scanning confocal microscope (Leica Microsystems, Heidelberg, Germany) equipped with an Acousto Optical Beam Splitter (AOBS). Images were acquired with a 63× oil immersion objective lens and image treatment was performed using the Image Processing Leica Confocal Software and ImageJ 1.47m Software (Wayne Rasband, Bethesda, MA).

2.5. Protein/lipid interactions on dot blots

Lipid dot blots were performed as previously described [41,43]. In brief, proteins were incubated overnight at 20 μM and room temperature, with the lipid blots. Lipid/protein interaction detection was made with anti-His antibody and revealed by the NBT/BCIP method.

2.6. PM-IRRAS and ellipsometry experiments on lipid monolayers at air–water interface

Polarization-modulation-infrared reflection-adsorption spectra (PM-IRRAS) were recorded on a Nicolet (Madison, WI) Nexus 870 spectrometer equipped with a HgCdTe (MCT) detector (SAT Poitiers, France) and cooled at 77 K by nitrogen liquid at a resolution of 8 cm^{-1} by coadding 600 scans. Details of PMIRRAS experiments were described in a previous paper [19]. PM-IRRAS spectra were normalized by the subphase spectrum or lipid monolayer spectrum.

Ellipsometry measurements were performed using a NFTElli2000 ellipsometer (Gottingen, Germany) equipped with a doubled frequency Nd:YAG laser at 532 nm with 50 mW power (for more details on ellipsometry see [41,44]). The spatial resolution was about 2 μm and the image size was 450 × 670 mm, with a 10× magnification lens. Thickness was determined using a mean value of 1.45 for the refractive index.

2.7. Preparation of small & large unilamellar and multilamellar vesicles

Dry films of DMPC, egg PC or asolectin (for small unilamellar vesicles, SUVs and large unilamellar vesicles, LUVs) were prepared from solutions in chloroform:methanol (4:1, v/v) evaporated under a stream of nitrogen and left under vacuum overnight to remove all traces of organic solvent. The lipid film was suspended in PBS pH 7.4 or D_2O and gently vortexed for a few minutes.

SUVs for ATR-FTIR experiments were obtained by sonifying the hydrated solution of lipid films in D_2O using a titanium rod sonifier (Vibracell, Sonics, Newton, USA) in an ice-water bath to avoid lipid thermal degradation. The traces of titanium were then removed by centrifugation (6000 rpm, 2 min).

To form LUVs, for calcein leakage experiments, dried film was hydrated with buffer containing calcein (70 mM in 1× TBS pH 7.4) and dispersion was run through five freeze/thawing cycles and passed through a mini-extruder equipped with two stacked 0.1 μm polycarbonate filters (Avanti, Alabaster, AL). The sizes of LUVs were determined to be around 120 nm by dynamic light scattering (DynaPro Nanostar, US). The lipid concentration was calculated by phosphate dosage [45].

MLVs (multilamellar vesicles) for NMR experiments were made of a mixture of asolectin and 1-$^2H_{31}$-palmitoyl-2-oleoyl-sn-3-phosphocholine (POPC-$^2H_{31}$ with a 4.5:0.5 ratio). Deuterated lipids were added in low quantity (10 mol%) to get enough deuterium NMR signal with a minimum perturbation of the membrane. Freeze-dried proteins were first solubilized in 80 μL of deuterium-depleted water (^1H_2O) and then mixed to the lipid mixture (~100 mM). After vortexing, the samples were subjected to 3 freeze-thaw cycles (1 min/10 min) to ensure complete equilibrium [46,47]. Lipid/protein molar ratio (*Ri*) of 50 was used for NMR.

2.8. ATR-FTIR spectroscopy

Polarized ATR-FTIR spectra were recorded on a Nicolet 6700 FT-IR spectrometer (Nicolet Instrument, Madison, WI) equipped with a liquid nitrogen cooled mercury–cadmium–telluride detector (ThermoFisher Scientific, San Jose, CA, USA), with a spectral resolution of 4 cm^{-1} and a one-level zero filling.

For the study of the interaction with supported bilayers, 10 μL of SUV samples were deposited for 5 min on a germanium ATR crystal in order to form one regular bilayer at the surface of the crystal. Since ATR spectroscopy is sensitive to the orientation of the structure [48], spectra were recorded with a parallel (*p*) and perpendicular (*s*) polarization of the incident light. All the orientation information is then contained in the dichroic ratio $R_{ATR} = Ap/As$, where Ap and As represent the absorbance of the considered band for the *p* or *s* polarization of the incident light, respectively (for more details see [49]). After D_2O washings, proteins were incubated for 10 min with the bilayer before washing with D_2O. For the mixed proteins/lipids, the SUVs were deposited for 10 min on the ATR-crystal to promote the formation of the bilayer and directly washed with D_2O. Two hundred interferograms, representing an acquisition time of 7 min, were co-added with a 4 cm^{-1} resolution.

For kinetic studies, the proteins in 25 mM Tris/HCl pH 8.0 were buffered with 1× PBS at pH 7.4 to a final concentration of 50 μM. Time 0 (T_0) of kinetics corresponded to pure proteins. Incubations were performed at 37 °C without agitation. Kinetics in the presence of DMPC SUVs was performed by adding 2.5 mM of SUVs. The first measurement was done after a 5 min drying of a 5 μL drop onto the germanium ATR crystal (Specac, Orpington, UK). All the aliquots generated during the kinetics were analyzed after 5 min of drying. One hundred interferograms, representing an acquisition time of 3.5 min, were co-added.

To determine the secondary structure element of each protein, ATR-FTIR spectra were analyzed with an algorithm based on a second-derivative function and a self-deconvolution procedure (GRAMS software and OMNIC software, ThermoFisher Scientific) to determine the number and wavenumber of individual bands within the spectral range 1485–1750 cm^{-1}, as described in our previous paper [41].

2.9. Solid-state NMR spectroscopy with MLVs

MLV samples (prepared with asolectin/d31-POPC as described in Section 2.7) with and without proteins were placed into an 80 μL ZrO_2 rotor (Cortecnet, Voisins-Le-Bretonneux, France). Deuterium NMR experiments were performed on a Bruker Avance III 800 SB spectrometer with a CP-MAS dual 4 mm ^1H/X DVT probe (Bruker, Wissembourg, France) at 122.8 MHz. Quadrupolar echo pulse sequence was used [50]. Typical acquisition parameters were as follows: spectral window of 500 kHz; π/2 pulse widths of 4 μs; and interpulse delays of 40 μs. A recycle delay of 2 s was used. Typically, 12,000 scans were recorded. A line broadening of 200 Hz was applied before Fourier transformation. Phosphorus NMR experiments were performed on a Bruker Avance DSX 500 WB spectrometer equipped with a PE-MAS triple 4 mm $^1H/^2H/^{31}P$ probe at 202.5 MHz by means of a Hahn Echo pulse sequence [51]. Static and magic angle spinning experiments were performed. Typical acquisition parameters were as follows: spectral window of 250 kHz (100 kHz with rotation); π/2 pulse widths of 2.75 μs; and interpulse delays of 30 μs. High power proton decoupling was performed during acquisition. A recycle delay of 5 s was used. 3000–6000 scans were recorded. A line broadening of 0–100 Hz was applied before Fourier transformation. Quadrature detection was used in all cases [46,47]. Samples were allowed to equilibrate ≥30 min at 25 ± 1 °C before the NMR signal was acquired.

2.10. Plasmon waveguide resonance (PWR) studies with supported bilayers

PWR spectra are produced by resonance excitation of conduction electron oscillations (plasmons) by light from a polarized CW laser (He–Ne; wavelength of 632.8 and 543.5 nm) incident on the back surface of a thin metal film (Ag) deposited on a glass prism and coated with a layer of SiO_2. Experiments were performed on a beta PWR instrument from Proterion Corp. (Piscataway, NJ, USA) that had a spectral angular resolution of 1 mdeg PWR spectra, corresponding to plots of reflected light intensity versus incident angle, can be excited with light whose electric vector is either parallel (*s*-polarization) or perpendicular (*p*-polarization) to the plane of the resonator surface (for more details on PWR see [52]). The egg PC lipid bilayer membrane was immobilized on the resonator surface of the prism by depositing 2 μL of a 10 mg/mL solution dissolved in butanol/squalene (95/5 v/v). The method used to make the lipid bilayers is based on the procedure by Mueller et al. to make black lipid membranes across a small hole in a Teflon block [53]. Briefly about 2 μL of the lipid solution is spread across the small Teflon block hole and immediately the cell sample compartment is filled with PBS. Spectra are then acquired for both polarizations and both spectral shifts with *p*- and *s*-polarization measured to ensure that a lipid bilayer was deposited with the proper orientation. This lipid bilayer is attached to the Teflon block by a lipid reservoir called plateau Gibbs border. Lipids in this reservoir can move in and out as imposed by the events occurring in the membrane (protein insertion, changes in lipid packing, etc.). The REF and SRPP proteins were either injected into the cell sample compartment containing the cell membrane in an incremental fashion or at a fixed concentration (kinetic measurements), and the spectral evolution followed in time. The kinetic data was fitted by a two-phase exponential association equation using GraphPad Prism.

2.11. Membrane leakage experiments with LUVs

Calcein-containing LUVs were made as described in Section 2.7. Free calcein was separated from the calcein-containing LUVs using size exclusion column chromatography (Sephadex G-100; Pharmacia) and elution with 1× TBS buffer. For the assay, the lipid concentration was set at 10 μM and protein concentrations were adjusted to *Ri* 1, 25, or 50. Fluorescence measurements were made with a POLARstar Omega microplate reader (BMG Labtech, Champigny-sur-Marne, France). The standard 96 well microtiter plate was shaken for 9 s, directly after the addition of all components but not during the measurement. Data were collected every 5 min at 25 °C using a $\lambda_{excitation}$ at 485 nm and $\lambda_{emission}$ at 540 nm. At the end of the assay, the complete leakage of LUVs was achieved by adding 5 μL of 10% Triton X-100 (Sigma) solution. The percentage of calcein release was calculated according to the following equation : $L(t) = (Ft - F0) / Ff - F0 \times 100$, where L(t) is the fraction of dye released (normalized membrane leakage), Ft is the measured fluorescence intensity at time t, and F0 and Ff are respectively the fluorescence intensities at times t = 0, and after final addition of Triton X-100. Each experiment was at least repeated 3 times.

3. Results and discussion

3.1. SRPP interaction with rubber particles is different than REF interaction

Rubber particles are composed of polyisoprene, proteins and a monolayer membrane as schematized in Fig. 1A. From early ellipsometric experiments, it was thought that the effects of proteins could be directly visualized on latex monolayers, as rubber particles are supposed to float at the air–water interface and form a one particle thick layer [9]. Unfortunately, by ellipsometry only a non-homogenous Langmuir film with an irregular thickness was observed (Fig. 1B). We then decided to focus our study of REF and SRPP on the interactions with various model membranes and subsequent effects on membrane organization. The latex produced by plant laticifers is a complex white cytoplasmic system, which may be easily separated by a simple centrifugation (Fig. 1C). Indeed, it contains mainly rubber and non-rubber particles, organelles, proteins and cytoplasmic C-serum [1]. REF and SRPP are not localized in the same phase of the latex, SRPP being washed away from the top cream (WRP), which concentrates the REF fraction and the LRPs (Fig. 1D). This can be explained by the fact that SRPP is mainly present on the small rubber particles (lower cream) or most probably easily washed from the particles. A previous report stated that latex osmotic lysis could release SRPP from the particles although most of REF remained associated with them [54]. We may therefore suspect a weaker interaction of SRPP with the particle membrane. In addition, a simple staining of the WRP with Nile red showed by fluorescence confocal microscopy a complete filling of the WRP with the dye, pointing out the homogeneous hydrophobic nature of the whole particle (Fig. 1E) and the potential of exchange and diffusion through this membrane. Moreover, the incorporation of DPPE-rhodamine was only visible on the outside of the particle, the free lipids therefore being subsequently integrated in the biomembrane surrounding the polyisoprene. This membrane has proven to be quite dynamic and let us think about the possibility of also adding proteins on it.

In order to investigate the interaction of REF and SRPP with different artificial model membranes, an affinity screen of various phospholipids was preliminary realized by dot blots (Fig. 2). Asolectin is a mixture of phospholipids extracted from soybean; the presence of mainly PC, PE, CL or PG, and PI was confirmed by ^{31}P NMR and thin layer chromatography (Supplementary Fig. S1). They are also the main phospholipid components of rubber particles [11]. Most of the lipids that we tested in this study reacted similarly towards both proteins. The weak reactivity of REF and SRPP towards DMPC on blots (whereas egg PC and POPC interact well) may be explained by the fact that this experiment was realized at room temperature below the transition phase of DMPC (23 °C), and the lipids are presented on the membranes in a non-organized state. This effect is not seen with DMPE and could also reflect a difference of affinity of the whole lipid. Note that all further experiments using DMPC were done at 25 °C. With this technique, it is not possible to discriminate a phospholipid favored in the interaction of REF or SRPP, but clearly both proteins had affinity for phospholipids.

3.2. REF has a stronger interaction than SRPP with lipid monolayers at air–water interface

In a previous work, we showed by ellipsometry that SRPP and REF could interact with DMPC or asolectin monolayers [41]. In this work we went further in the characterization of this interaction by first looking at the secondary structure of the proteins in the presence of lipids using polarization-modulation-infrared reflection-adsorption (PM-IRRAS) spectroscopy at the air–water interface (Fig. 3A). The 2 proteins alone injected in the subphase were very surface active, quickly moving to the air–water interface. The surface pressure was measured at 14 mN/m and 12 mN/m for REF and SRPP, respectively. Thick films were formed at the air–water interface as observed on the ellipsometric images (Fig. 3B top panels). The observation of both amide bands (I and II) in the range 1750–1450 cm^{-1} proves the presence of the proteins at the air–water interface. REF was the more reactive protein, whereas SRPP was less reactive, according to the intensity of the amide I bands, in agreement with the lower thickness measured for SRPP in ellipsometry. For both proteins the PM-IRRAS spectra (Fig. 3A top panel) show a broad amide I band, indicating that several secondary structures (turn, α-helices, random coils and β-sheets) coexist. We previously demonstrated that REF has amyloid properties, forming parallel

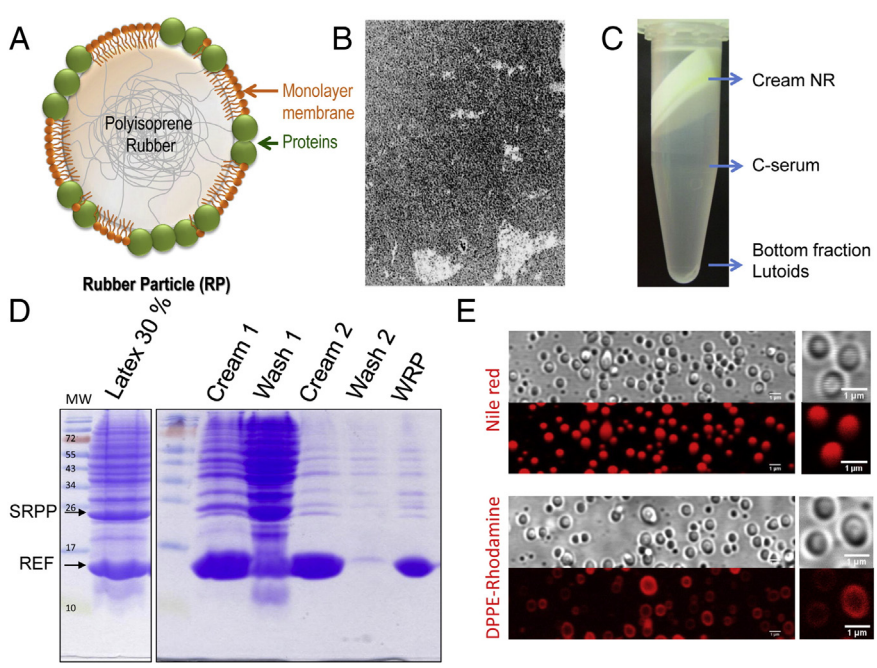

Fig. 1. Latex and rubber particles. A) Schematic representation of a rubber particle. B) Ellipsometric image of ammoniated latex. C) Observation of non-ammoniated latex after centrifugation at 20,000 *g* for 30 min. D) Full protein content of non-ammoniated latex before and after centrifugation and washing. Rubber particles of latex (RP) and washed rubber particles (WRP) were denatured, run on a 15% SDS-PAGE and stained with Coomassie blue. E) Staining of WRPs with Nile red or DPPE-rhodamine followed by an observation by confocal microscopy.

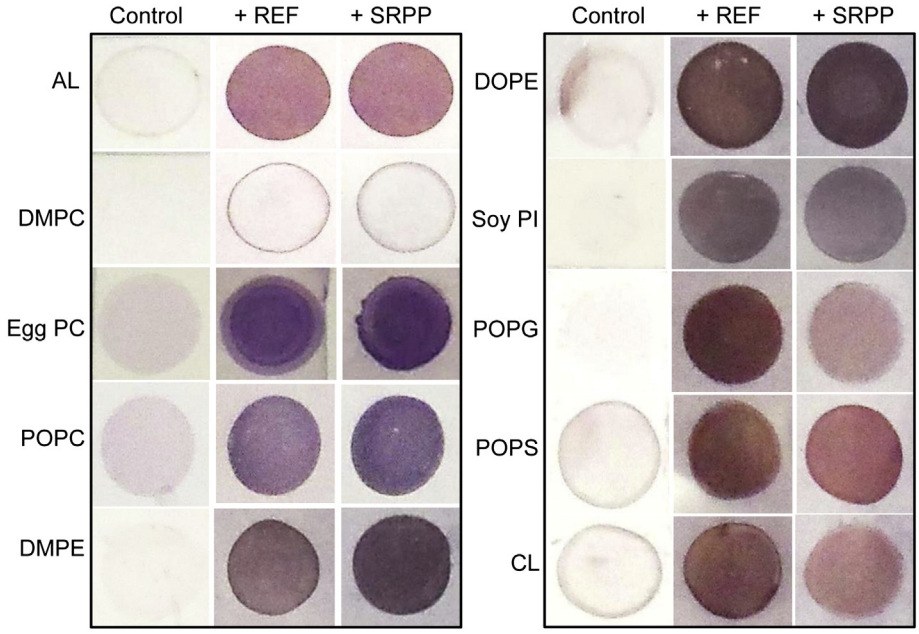

Fig. 2. Interaction of REF and SRPP with specific phospholipids on lipid dot blots. Bulk lipids were deposited as a drop/dot on a blot and then incubated overnight with 20 μM proteins in 1× PBS at room temperature. Controls were only incubated with PBS. The presence of the proteins interacting with the fixed lipids was revealed using specific anti-histidine antibody and red dyes. Abbreviations: asolectin, AL; phosphatidyl choline, PC; cardiolipin, CL; phosphatidyl ethanolamine, PE; phosphatidyl serine, PS; phosphatidyl inositol, PI; phosphatidyl glycerol, PG; 1,2-dioleoyl-sn-glycero, DO; 1,2-dimyristoyl-sn-glycero, DM; 1-palmitoyl-2-oleoyl-sn-glycero, PO.

β-sheets in solution [41], which is not similar at the air–water interface. In the presence of a DMPC monolayer at 28 mN/m (Fig. 3A bottom panel) only the amide bands of REF could be detected, and no signal was detected for SRPP. The control DMPC monolayer spectrum is presented in Supplementary Fig. S2. An increase of the surface pressure (+9.8 mN/m) was only observed after injection of REF. REF interacts strongly with DMPC and clearly modifies the lipid monolayer. A large accumulation of the REF protein is revealed by the increase of the film thickness at the air–water interface (+47 Å). In comparison, we observed that SRPP slightly increased the thickness of the DMPC monolayer (+9 Å) [41]. Like in the air–water interface alone, no strong variation of the secondary structure of REF in the presence of the lipid monolayer was observed. The same broad amide I band was detected. In contact with lipids, no preferential REF orientation is observed. The results lead to the conclusion that the interaction of REF with a lipid monolayer at air–water interface is stronger than that of SRPP.

3.3. The structure of REF changes in the presence of lipid bilayer as model membrane

To try to elucidate the secondary structure of both peptides interacting with membranes, we studied their interaction with planar

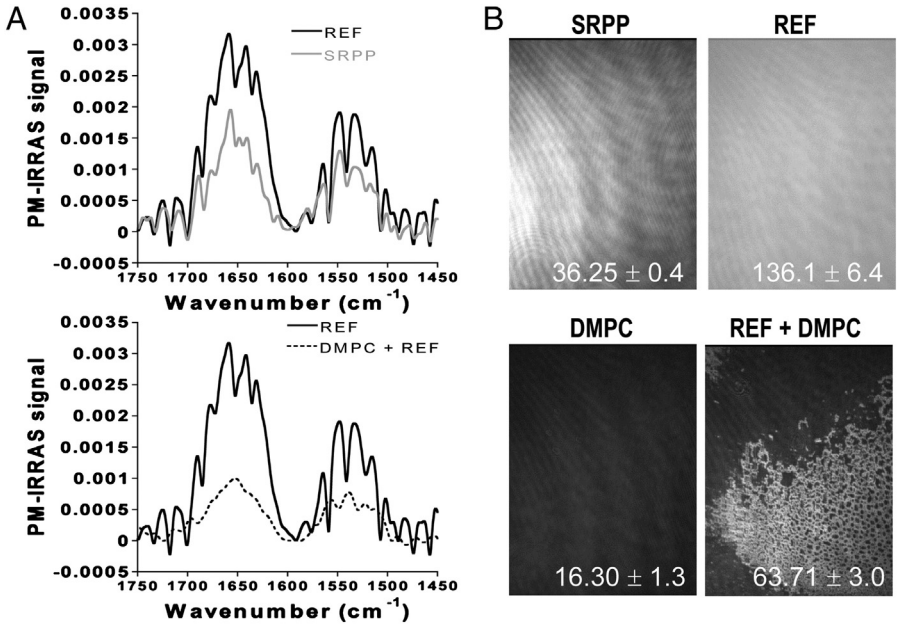

Fig. 3. REF has a stronger interaction with DMPC Langmuir monolayer. A) PM-IRRAS spectra of proteins alone at the air–water interface (top) and REF in the presence of a DMPC monolayer at 28 mN/M (bottom). No signal was observed with SRPP. B) Ellipsometric images corresponding to the conditions described in A. The layer thickness (Å) is reported in white on each image. Experiments were performed in 1× PBS, the concentration of the protein was 1 μM and the temperature was set to 25 °C.

bilayers by polarized ATR-FTIR spectroscopy. Small unilamellar vesicles (SUVs) of DMPC were deposited on ATR crystal and the formation of the bilayer was followed by the absorbance of the antisymmetric (2924 cm^{-1}) and symmetric (2853 cm^{-1}) stretching modes of methylene groups (results not shown), as described by Castano and Desbat [49]. The position of the band and the dichroic ratio (R_{ATR} = Ap/As) allow the conclusion that a supported bilayer was formed at the surface of the ATR crystal, properly oriented and with a slight organization of the chain. First, the proteins at 10 μM were incubated on this bilayer and carefully washed with D_2O. Only the amide I band of REF was detected, again no SRPP could be detected after washing (Fig. 4A). The 1730 cm^{-1} band is assigned to the C═O stretching of the phospholipids. No variation of the position of the ν_{as} and ν_s of CH_2 was observed (results not shown), indicating that the acyl chains remained only slightly organized. In another set of experiments, the proteins were directly mixed with the lipids before the formation of the SUVs. Interestingly, SRPP inhibited the formation of SUVs and so these experiments were only possible with REF (Fig. 4B). Spectra of REF added either before or after DMPC bilayer deposition were quite similar, indicating a strong interaction with the membrane. To further investigate REF and SRPP lipid interaction, we have performed the same experiments using egg PC SUVs at higher protein concentration (50 μM). With these new conditions, the presence of SRPP was detected at the lipid interface, but with a far smaller peak than REF. REF underwent a similar structural change as that observed with DMPC (Supplementary Fig. S3). In conclusion, the interaction of SRPP with bilayers is therefore weaker than that of REF. Table 1 lists the percentage of each secondary structure component of REF in solution or upon interaction with DMPC bilayers. The structure of REF interacting with lipids is quite different from its structure in solution. The aggregation of REF, as amyloid-like protein, was poorly detected (small content of β-sheet). REF was added to the membrane as monomer, and in contact with lipids around 33% of the bound peptide was unstructured (random coils), 15% was helical (α-helices) and only 27 or 21% was involved in β-sheet structures. It clearly appears that the interaction with lipid modifies the aggregation process of REF.

Then, the third experiment we performed with integral DMPC SUVs was to follow the kinetics of the protein structural changes. Proteins at 50 μM were incubated at 37 °C with DMPC SUVs (2.5 mM; $Ri = 50$), and the structural changes were analyzed by ATR-FTIR upon SUV/protein mixture deposition on the ATR crystal (Supplementary Fig. S4). If the presence of SUVs does not really modify the structure of SRPP, this is totally not the case with REF. It clearly appears that REF amyloidogenesis is inhibited by the SUVs (see Table 1 and Fig. 4C for the relative β-sheet content of REF). The three different experiments performed with REF indicate a decrease in β-sheet structures and hydrophobic domains and a neat increase in random coils and α-helices. Apart from the impossibility of forming SUVs in the presence of SRPP, SRPP structure does not seem to be modified by the presence of SUVs. Thus DMPC or egg PC bilayers have only a major effect on REF structure and aggregation process.

3.4. The membrane integrity may be differently modified by REF and SRPP

Next we investigated the effects of proteins on lipid membrane organization. To this end multilamellar vesicles (MLVs) of mixed asolectin and $^2H_{31}$-POPC (10%) were prepared and ^{31}P and ^2H solid-state NMR was undertaken, to monitor changes in membrane structure and dynamics at membrane surface (^{31}P of phosphate head group) and bilayer core (^2H of hydrocarbon perdeuterated chains). Results in Fig. 5 show the effect of the presence of REF and SRPP in MLVs at $Ri = 50$. Deuterium powder pattern spectra are shown in Fig. 5A, in the absence and presence of both proteins. They are characteristic of micrometer-size MLVs in their fluid (liquid disordered) phase at 25 °C [46]. It is in agreement with the presence of unsaturated lipids (PC, PE, PI, PG or CL) contained in asolectin. Central doublet reports on the very disordered (low rigidity) bilayer center (acyl chain methyl terminal), whereas the doublets detected at ±13 kHz report on the more rigid membrane interface (positions near the glycerol backbone) [55]. SRPP slightly affects the rigidity as reported by $^2H_{31}$-POPC, whereas REF reduces the pattern width, especially for labeled positions in the hydrophobic core near the bilayer interface. Overall membrane rigidity can be calculated from spectra [46,47,55] and results indicate a 10% increase in fluidity promoted by REF. No significant variation of fluidity was observed with SRPP. Fig. 5B shows head group modifications using ^{31}P NMR.

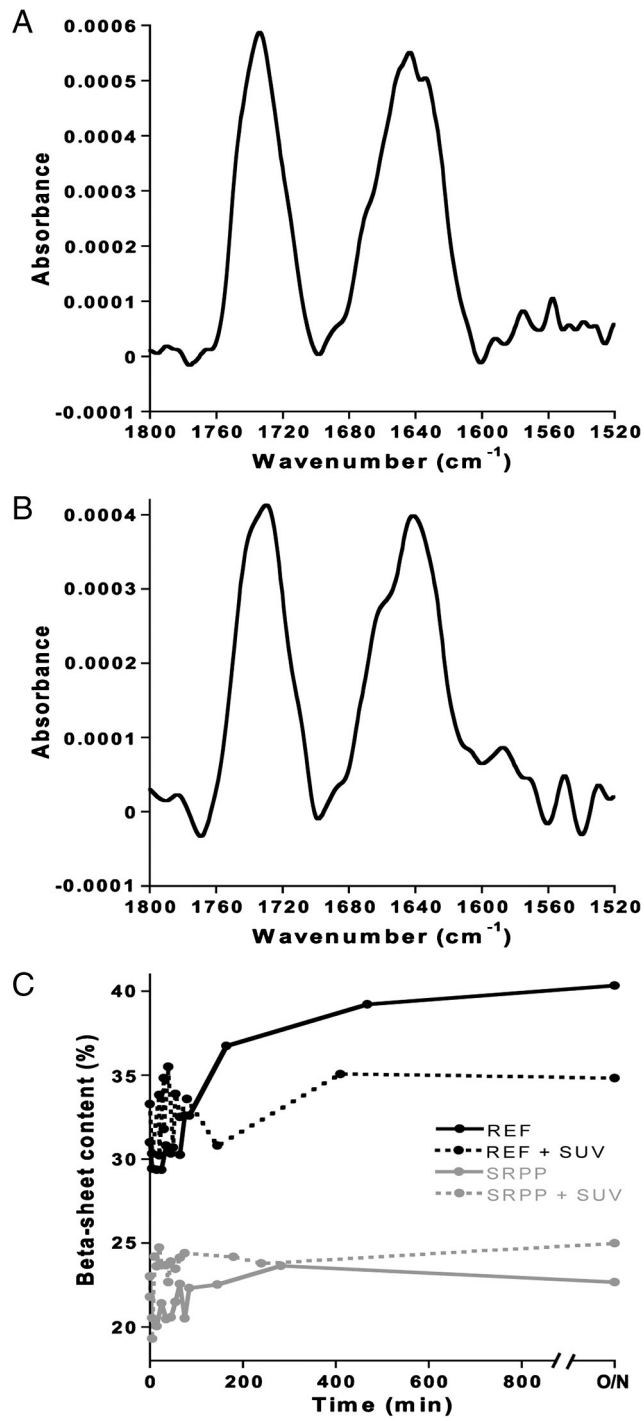

Fig. 4. REF and SRPP structure in interaction with DMPC bilayers. A) *p*-polarized ATR-FTIR spectra of REF interacting with supported planar bilayer created from DMPC SUVs deposited on a Ge crystal. B) *p*-polarized ATR-FTIR spectra of REF prepared in DMPC SUVs with a ratio of 1:50 ($Ri = 50$) spreading onto the ATR crystal. C) Kinetics of β-sheet formation was followed by ATR-FTIR with or without integral DMPC SUVs. REF and SRPP were at 50 μM in 1 × PBS and 37 °C, SUVs were added at 2.5 mM ($Ri = 50$). Independent kinetics is presented in Supplementary Figure S4. Quantified results are presented in Table 1.

Table 1
ATR-FTIR analyses of REF and SRPP with DMPC small unilamellar vesicles (SUVs) or bilayers.

Secondary structure element	Amide I (cm^{-1})	Relative comparative (%)					
		REF[a]	REF on bilayer[b]	REF in bilayer[c]	REF with SUV[a]	SRPP[a]	SRPP with SUV[a]
Aggregation	1614	6.79	9.28	7.83	4.24	9.25	7.99
β-sheets	1630	40.33	27.28	21.52	34.82	22.67	24.98
Random coils	1646	20.85	32.36	34.53	24.05	21.39	22.18
Helices	1657	10.71	14.08	17.72	13.95	22.12	21.72
Turns	1670	10.21	10.81	13.34	13.28	12.12	12.79
Hydrophobic domains	1685	11.11	6.16	5.04	9.66	12.45	10.34

Accuracy is estimated to be within ~2.5% and measurement temperature was set at 25 °C.
[a] REF and SRPP were incubated in PBS 1× at 50 μM and 37 °C overnight. DMPC SUVs were incubated with proteins in the same conditions at $Ri = 50$. Spectra of aggregates were recorded after drying on the crystal.
[b] DMPC SUVs were first deposited on the ATR crystal for membrane formation, before protein addition at 10 μM. After washings in D_2O, spectra were recorded. No amide I signal was observed in the same experiment in the presence of SRPP.
[c] REF was mixed with DMPC before SUV formation in a 1/50 ratio ($Ri = 50$). SUVs with proteins were fusionned on the ATR crystal, and then washed in D_2O before recording spectra. SRPP incorporation into lipids did not permit the formation of SUVs.

Here all phospholipids in asolectin contribute to the overall axially symmetric spectral shape, which, in the absence of proteins, pictures a micrometer-size MLV in the fluid phase (broad spectrum spanning a [−20, +40 ppm] width) [46]. A sharp peak accounting for ~5% of the total spectrum is detected near 0 ppm. Because NMR is quantitative, this indicates that 5% of the total system is under the form of very small vesicles or micelles that tumble so fast that they average the chemical shielding interaction to zero. In the presence of SRPP, the overall shape is basically unchanged except for the appearance of sharp lines (~10% of total area near 2–3 ppm). This suggests the formation of a small additional fraction of small vesicles or micelles. Because we can measure chemical shifts of −1, 0, 2.4 and 4.2 ppm, the presence of these small isotropic lines suggests that all classes of lipids (PC, PE, PI, PG or CL) are solubilized as a small fraction of the total lipid membrane. REF modifies to a much larger extent the powder spectrum. Two sharper peaks of about 16 and 4 ppm dominate the spectrum. Again, this indicates that part of the MLVs may be under the form of small lipid assemblies that tumble very rapidly. Interestingly, isotropic lines do not appear in the deuterium spectrum recorded on the same sample from the POPC viewpoint (Fig. 5A, bottom). This indicates that if a possible membrane "solubilization" occurs, it is not accomplished with PC lipids.

In order to further assess the "solubilization" issue as suggested by wide line ^{31}P and ^{2}H NMR (Fig. 5), we performed an experiment that consists in spinning the NMR rotor very quickly (12 kHz) at the magic angle (MAS; Fig. 6B–C). This converts a wide line spectrum, as observed for large aggregates or solids dominated by the chemical shielding anisotropy (CSA), into sharp lines; the sample remaining in the assembled/organized form. Also of interest, an isotropic line, as in liquids or micelles, will not change its position under MAS conditions. Such an experiment was performed on NMR samples in the presence and absence of REF (Fig. 6B–C). The wide line spectrum observed for asolectin MLVs alone (Fig. 6C) mainly shows under MAS a "sharp" line corresponding to superimposition of isotropic PC, PE, PI and CL or PG resonances. A liquid-

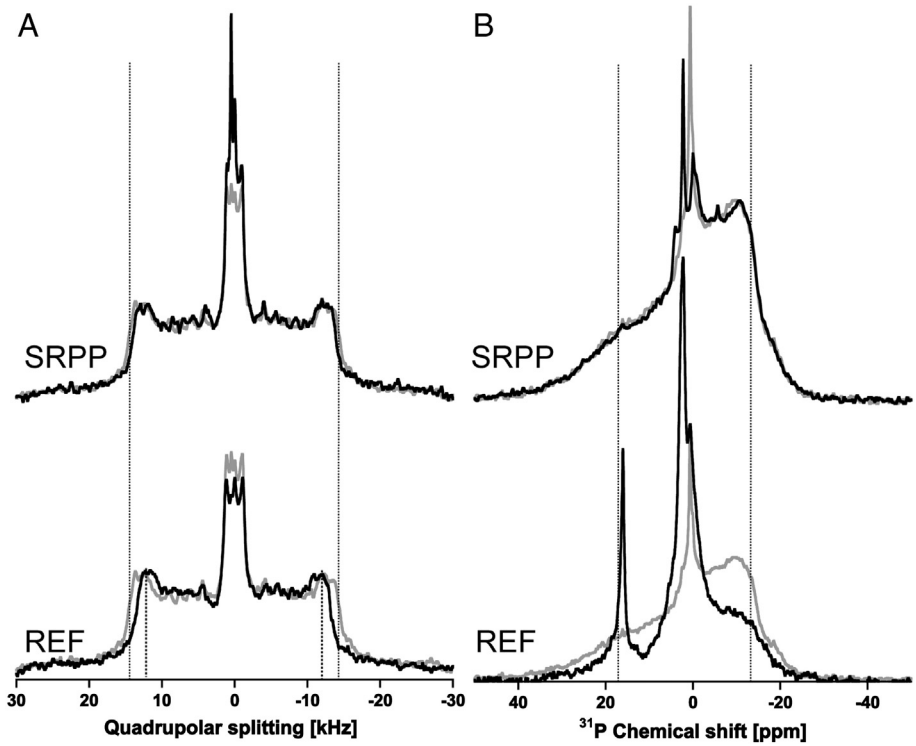

Fig. 5. Different interactions of REF and SRPP with MLVs by solid-state NMR. A) ^{2}H NMR spectra of MLVs alone (gray) or in the presence of SRPP (black, top panel) or REF (black, bottom panel). B) ^{31}P NMR spectra of MLVs alone or in the presence or REF or SRPP. MLVs were made of a mixture of asolectin and POPC-d31 (4.5:0.5). Freeze-dried REF and SRPP were added to the lipids at $Ri = 50$. Experiment was performed at 25 °C.

state ^{31}P NMR spectrum of pure asolectin (Supplementary Fig. S1B) indicates a better resolution and identification of the different lipid species according to reported chemical shifts [47,56]. When spinning the sample containing REF (Fig. 6B), the 16 ppm line as observed with static wide line NMR (Fig. 6A) is still detected and appears sharper. Other sharp lines at approximately 2, 3, and 4 ppm are also detected with the major line representing PC lipids at −0.8 ppm. The chemical shift coincidence of sharp lines obtained in MAS conditions (at 16, 4, 3, 2 ppm) with those obtained under wide line NMR clearly indicates that MAS was not efficient in averaging out the chemical shielding anisotropy, that is obtained with large MLV, because there was no longer CSA to average out. This suggests that in the presence of REF, "solubilized lipids" may appear and behave as if they were in organic isotropic solution. This observation strongly suggests that REF could promote a micellization-like phenomenon. There is also another phenomenon that deserves a comment. The 16 ppm resonance, which is observed in the presence of REF, is unusual in ^{31}P NMR of lipids, except for very peculiar surroundings of the phosphorus nucleus. Phosphate chemical shifts (ATP, ADP, phospholipids) usually occur in the [+5, −20 ppm] range. Such a positive chemical shift for phosphate lipids can occur upon binding to a molecular species that induces a strong chemical shift effect or for phosphonates, where the presence of a phosphorus–carbon bond leads to phosphorus resonances near 20 ppm [57]. Because asolectin contains no phosphonate, there may be a specific clustering with aromatic amino-acids of REF that may produce such a huge chemical shift on phosphate resonances. To conclude, results clearly show here that membrane integrity may be differently modified by REF and SRPP.

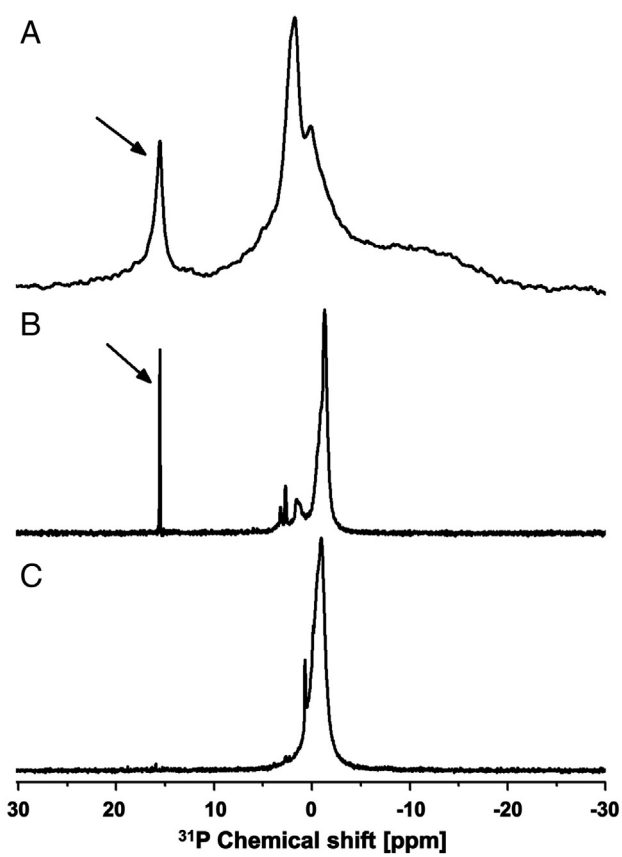

Fig. 6. ^{31}P NMR of asolectin MLVs (containing 10% $^{2}H_{31}$-POPC) under magic angle spinning (MAS) conditions. A) Static spectrum of REF ($Ri = 50$ same as Fig. 5B bottom black), showing a superposition of wide line featureless patterns (micrometer-size MLVs) and sharp lines. B) MAS spectrum at 12 kHz of REF sample ($Ri = 50$), the sharp line (arrow) detected one static spectrum at about 16 ppm is also observed at that same frequency after spinning. C) MAS spectrum at 12 kHz of asolectin vesicles in the absence of REF. Experiments were performed at 25 °C.

3.5. The interaction of SRPP and REF with an egg PC lipid bilayer investigated by PWR

PWR has been proven useful to follow the interaction of membrane active peptides with planar lipid membranes both in terms of the affinity of those interactions as well as the kinetics and effects on lipid organization (to cite a few examples:[58–61]). Herein PWR was used to monitor the interaction of SRPP and REF with a planar solid-supported egg PC lipid bilayer. After formation and stabilization of the lipid bilayer (no spectral changes or very small changes observed over time for both polarizations) the protein was added to the PWR cell sample compartment in an incremental fashion. For each concentration, spectral changes were followed, the resonance minima positions measured and changes in spectral depth followed. The system was left to equilibrate (no or very small spectral changes observed) before adding the following protein aliquot.

As shown in Fig. 7 (panels A and B), SRPP addition leads to a large increase in the spectral depth for both polarizations, starting at very low protein concentrations (100 pM). An increase in spectral depth is mainly associated with an increase in the membrane thickness, indicating that the protein is interacting with the membrane, starting at very low concentrations. As for the resonance minima position there is a great increase in the minimum at 100 pM (15 and 16 mdeg for *p*- and *s*-polarizations, respectively) indicating that there is an overall increase in the refractive index of the lipid membrane which is a direct consequence of a mass augmentation coming from the protein itself. Upon addition of increasing concentrations there are shifts to smaller angles (up to around 100 nM) for both polarizations. Shifts to smaller angles are due to a mass decrease. Since protein is being added to the membrane this decrease in mass of the proteolipid system can only be explained by a lipid reorganization that leads to a smaller bilayer density (mass per surface). The addition of increasing protein concentrations leads to positive spectral shifts and even to a deformation of the spectra occurring at 20 μM. Such spectral deformation with the appearance of a shoulder in the right side can be attributed to heterogeneity of lipid and/or protein organization with the formation of domains of higher mass. Comparable spectral signatures have been observed in previous PWR for lipid bilayers whose composition was reported to form domains [52,62] and upon the action of amyloid peptides with the lipid membrane [59]. It is worth to notice that SRPP addition produced much higher spectral shifts in the *s*- than in the *p*-polarization (29 and 98 mdeg for *p*- and *s*-polarization at 20 μM, respectively). Such anisotropic response cannot be solely explained by lipid rearrangement, whose natural axis of symmetry is opposite (higher refractive index and so higher resonance shifts in the *p*-polarization than in the *s*-polarization). Therefore this indicates that the protein organizes itself in the membrane in an anisotropic fashion with its long axis parallel to the membrane surface, probably because the protein possesses an anisotropic structure (such as a cylinder).

Kinetic measurements of protein interaction with the membrane were performed that allow one to follow the changes in the resonance minimum position with time. Such measurements can only be performed with one of the polarizations, thus we have chosen the *s*-polarization because this resonance is sharper (allowing a better evaluation of the resonance minimum position) and because the spectral change induced by the protein is larger and the response was less variable than with the *p*-polarization (where more variation in the direction of the shifts was observed). The addition of SRPP to the membrane (20 μM, final concentration in the PWR cell) leads to a very sharp increase in the resonance angle within a very short period of time followed by a plateau (Fig. 7, panel C). The data could not be appropriately fitted by a one-phase exponential association model but was well fitted by a two-phase exponential association (with one fast and one slow event). This indicates that SRPP interaction does not follow a simple binding but that more than one phenomenon is occurring simultaneously in the binding process: more than one population of proteins (monomer versus oligomer) and/or two

distinct interaction sites/modes in the membrane are possible explanations. A fast kinetic rate constant of $30.8 \pm 3.7 \times 10^{-3}\ s^{-1}$ and a slow one of $1.49 \pm 0.05 \times 10^{-3}\ s^{-1}$ were obtained from the fit.

Regarding REF, while the first addition of protein also leads to a great increase in the spectra depth reflecting an increase in the bilayer thickness, like that observed with SRPP, further protein addition leads to a different response. Incremental REF addition to the bilayer leads to overall negative spectral shifts especially for the *p*-polarization where a total negative shift of about 40 mdeg was observed upon incremental addition of protein to a final concentration of 20 μM (Fig. 7, panels D and E). Since protein is being added, an increase in mass should be observed and consequently an increase in the resonance minimum position. This negative spectral shift is related to a reorganization of the membrane leading to a decrease in the overall mass of the system: lipid being removed from the membrane to the buffer in the form of micelles or from the bilayer center to its edges called plateau Gibbs border (lipid reservoir that exists in the contact point of the bilayer with the PWR Teflon cell). In addition to the differences in the direction of the spectral changes induced by each protein, the anisotropy of their response (comparison between the shifts in the two polarizations) is also completely different. In contrary to what was observed with SRPP, spectral shifts observed with *s*-pol were smaller (for 20 μM a negative shift of 18 mdeg was observed) than those observed with *p*-polarization. Additionally, spectral changes following each incremental addition were quite irregular in terms of the direction and magnitude, especially for the *s*-pol and for higher protein concentrations. For that reason, kinetic data with this protein performed with the *p*-polarization was rather non-exploitable since large variations in the magnitude and direction of the resonance minimum position were observed. It seems that the interaction of REF with the membrane leads to two processes whose contribution varies upon protein concentration: 1 — the protein interaction with the membrane, that leads to an increase in mass and positive spectral shifts; 2 — the lipid reorganization following the membrane interaction with lipid micellization and/or change in lipid mass/surface, which leads to negative spectral shifts. These observations therefore confirm NMR results.

An estimative value of the apparent affinity constant for the two proteins to the membrane based on hyperbolic fits of the resonance minimum position shifts as a function of concentration (using *p*-polarization data for REF and *s*-polarization data for SRPP) indicates that REF has an apparent affinity to the membrane in the low nanomolar order, about 100 times higher than SRPP (Supplementary Fig. S5). This is a general estimate since, especially for higher protein concentrations, the PWR spectra response was not totally equilibrated which is essential for an accurate determination of the affinity constant.

3.6. REF and SRPP cause leakage of egg PC LUVs

As REF seemed to have a drastic effect on all the membranes previously tested, we suspected that it probably also causes leakage or forms pores. To check this hypothesis, large unilamellar vesicles (LUVs of diameter about 120 nm) of egg PC, encapsulating calcein were employed. Contrary to rubber particles, which have a highly hydrophobic interior, LUVs have a bilayer with a very hydrophilic content that would certainly favor leakage. We indeed observed neatly the release of calcein and the consequent increase in fluorescence, due to the destabilizing effect of REF on the LUV bilayer but also of SRPP (Fig. 8). Surprisingly, SRPP exerted a stronger effect than REF even at low concentrations (Fig. 8A). Its effect was instantaneous and clearly different from the normal effect usually observed during the insertion of a protein, like that observed for REF. REF provokes leakage very quickly (no lag time was observed), in a time- and dose-dependent manner (Fig. 8B). But SRPP effect is nearly two times higher than REF effect (Fig. 8C). We may suppose that REF also initiate aggregation outside the LUV. This could explain that less monomers or oligomers are free to penetrate, to organize into the membrane and to induce leakage. If a pore is formed, it can also be transitory. For SRPP, the accumulation on the LUV membrane causes instant rupture, by weakening the LUV or creating cracks or defaults into the membrane. This effect is massive and certainly correlated with the fact that SRPP is able to inhibit the formation of SUVs when we try to incorporate the protein into the SUV (Section 3.3). This action was absolutely not observed on planar membranes or MLVs and could be attributed to a "carpet" effect [63]. A particular membrane curvature could allow a better protein binding. This may also reflect the preference of SRPP for binding to smaller RPs. It could explain why SRPP cannot be found on large rubber particles or are easily washed from them. The constraint could be driven by the

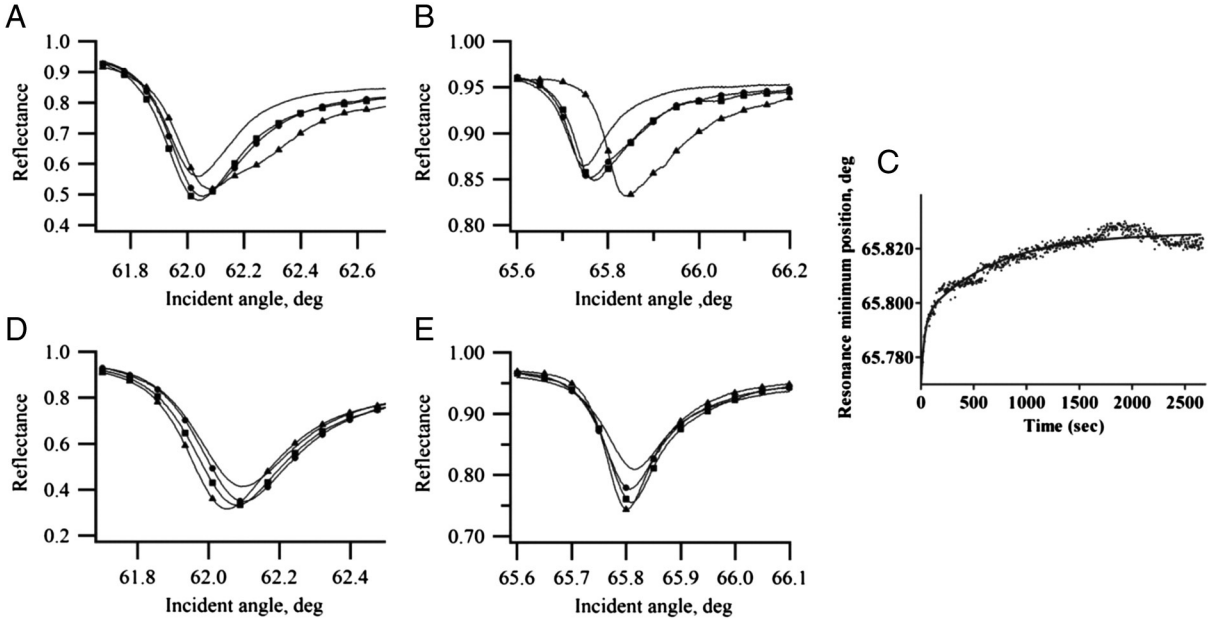

Fig. 7. Interaction of SRPP and REF with an egg PC bilayer followed by PWR. Panels A and B refer to the spectral changes induced by the addition of SRPP at 100 pM (●), 100 nM (■), and 20 μM (▲) to the lipid bilayer (solid line) obtained with *p*- and *s*-polarizations, respectively at the equilibrium (details about rate constant determination and their values are presented in the text). Panel C presents the changes in resonance minimum position, measured with the *s*-polarization, observed upon addition of 20 μM of SRPP to the bilayer. Panels D and E correspond to the same conditions as panels A and B but for REF protein. Experiments were performed in 1× PBS at 25 °C.

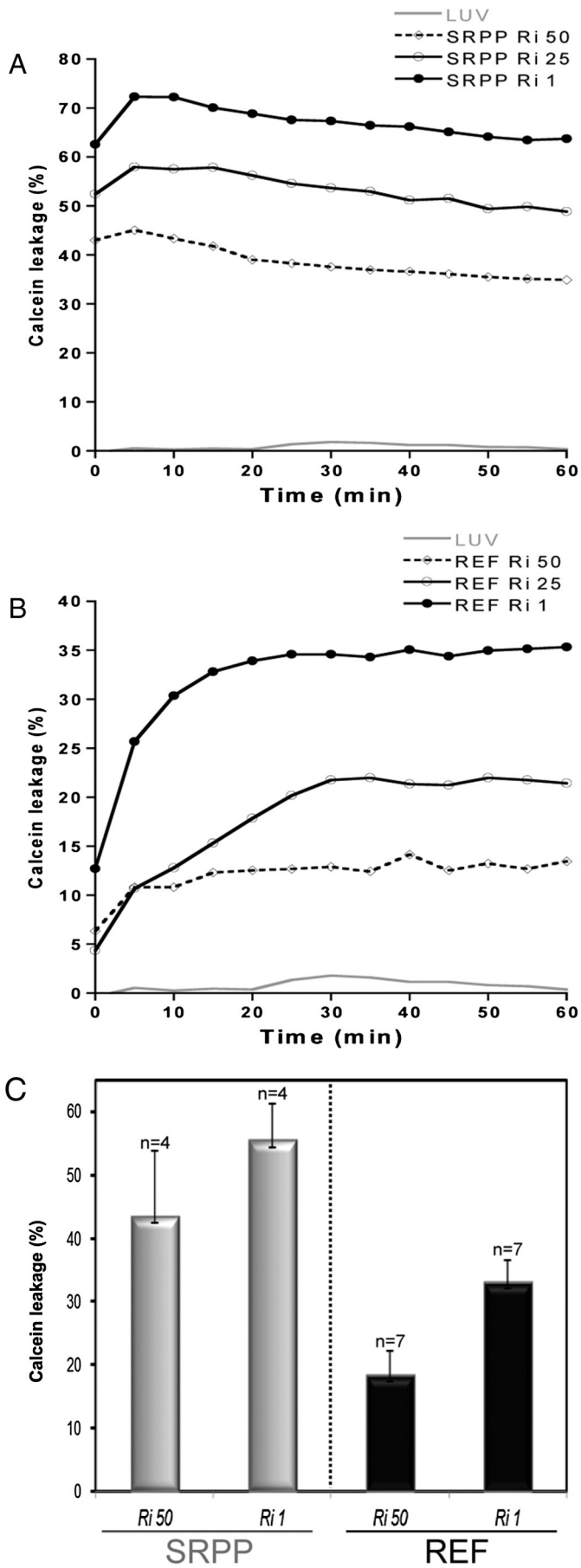

Fig. 8. SRPP and REF induce calcein release from egg PC LUVs. Kinetics of fluorescence release of SRPP (A) and REF (B) in the presence of calcein LUVs at *Ri* 1, 25 or 50. C) Quantification of calcein leakage of REF and SRPP at $Ri = 50$ and $Ri = 1$ (10 μM) after 1 h incubation in 1× TBS at 25 °C. Results are presented as mean ± standard deviation of independent experiments (n).

orientation of SRPP arrangement at the surface of lipids and the availability of phospholipid headgroups. The nature of liposome leakage greatly differs between the two proteins, again reinforcing the idea that the proteins act very differently on the membrane both in terms of affinity and induced membrane reorganization.

4. Conclusion

With this study, the interactions of both REF and SRPP with various model membranes were investigated, with a good convergence in terms of the results obtained. From our results, two different models of REF and SRPP interactions with the rubber particle biomembrane can now be proposed (Fig. 9). SRPP could largely cover the small rubber particle surface in an oriented anisotropic manner (Fig. 9A). The interaction with SRPs could be favored by an appropriate membrane curvature. In addition, it is interesting to note that SRPP is negatively charged (−6), but still interacts with negatively charged lipids (PG, PI). Therefore the hydrophobic nature of REF and SRPP plays an important role in the membrane interaction, as it has been shown for negatively charged antimicrobial peptides that bind to negatively charged lipid membranes [64,65]. Such an interaction was also shown to stabilize very small vesicles (30 nm) from large MLV by a process referred to as "electrostatic wedge", the hydrophobic interaction acting first to internalize negatively charged peptides, and then electrostatic repulsion with negatively charge lipids induced a highly curved membrane surface and stabilized small vesicles [64]. REF has clearly a stronger interaction, referring to binding, insertion and probably also auto-assembling inside the membrane (Fig. 9B). We previously reported such kind of interaction, with another amyloid protein which we called "raft-like" insertion [63]. In addition we noticed also that REF may be able to extract and sequester lipids from the membrane, possibly generating small micelles. As a recent study however stated that REF was equally present on both LRP and SRP [66], it can then be postulated that REF could be able to insert in both types of particles. In both cases REF and SRPP with the lipid monolayer contribute to the colloidal stability of latex, by forming a dense proteolipidic monomembrane.

We may now wonder why such homologous proteins may differ so much in their interaction with membranes. REF, as an amyloid protein, already presented a different structure. But its interaction with membrane clearly stabilizes the protein, inhibiting the amyloid state and aggregation, whereas this aggregation state could be of particular importance during coagulation. Very few "amyloid-like" proteins have been described in plants [67–69], but it is highly probable that numerous amyloid proteins fulfill a wide range of functions in the plant kingdom. In hevea, only microfibrils in the lutoids have been reported, but the proteins responsible of their formation are not yet identified [70]. The presence of amyloids could be of particular interest for the plant, as many amyloids are described as having antimicrobial, antifungal or antiviral properties [71]. REF and SRPP belong to a stress-related protein family [41] and their expression is clearly inducible by stress (e.g. tapping, tapping panel dryness syndrome) [54]. Their strong permeabilizing ability would surely help in eliminating pathogens trying to penetrate the bark.

In the case of REF we may also imagine that its interaction not only with lipids but also with polyisoprene could help in the "branching" process. Proteins are thought to be linked at the ω-terminal (the *trans* initiator group) of the polyisoprene while the phospholipids could be linked at the α-terminal phosphate group of the linear polymer chains [23,24]. From our results, we may also suppose multiple interactions (protein–lipid–polymer), these could effectively modulate the gel forming capacity and/or the molecular weight of natural rubber.

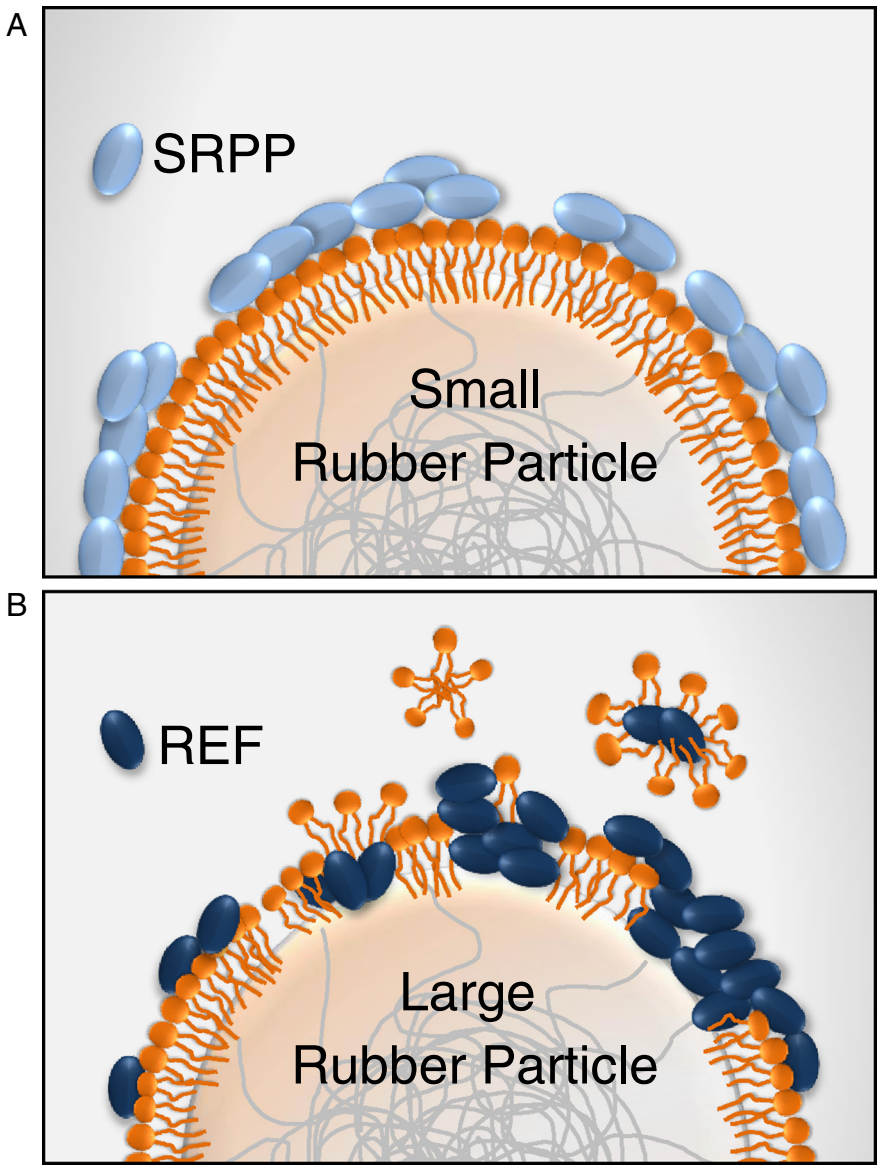

Fig. 9. Proposed models of REF and SRPP interactions with membrane. A) SRPP acts by "covering" small rubber particles. This interaction with the lipid headgroups could orientate the protein at the interface, creating anisotropy. B) REF may interact with the lipid by binding first and then inserting into the membrane. The aggregation properties of REF coupled to its lipid affinity may also refer as a membrane penetration termed "protein raft". Removal of some lipids from the membrane could be achieved by micellization.

Acknowledgements

KB and YE acknowledge the "Agence Nationale pour la Recherche" for their Post-Doctoral Researcher Fellowship (ANR Polyterp; ANR-10-CD2I-08). We thank Pr. Christophe Cullin (IBGC, Bordeaux) for kindly allowing us access to his microplate reader. Financial support from the TGIR-RMN-THC Fr3050 CNRS for conducting the research is gratefully acknowledged. The Aquitaine Government is also thanked for financial support to build the NMR platform. We are grateful to Michelin (Clermont-Ferrand, France) for providing latex samples from Brazil.

Author contributions

KB designed the study, performed the experiments and wrote the paper. SL performed ATR-FTIR, PM-IRRAS, ellipsometry and SUV experiments. YE and JT prepared the WRPs and performed the confocal microscopy. VZ carried out the NMR experiments. SH made the calcein-LUVs. IA performed the PWR experiments. KB, SL, IA, FP, YE, JT, VZ, ED, and SH analyzed the data and critically read the paper. FP funded and supervised the study.

Conflict of interest

The authors declare no conflict of interest.

Appendix A. Supplementary data

Supplementary data to this article can be found online at http://dx.doi.org/10.1016/j.bbamem.2013.08.025.

References

[1] J. d'Auzac, J.L. Jacob, H. Chrestin, The composition of latex from *Hevea brasiliensis* as laticiferous cytoplasm, in: J. d'Auzac, J.L. Jacob (Eds.), Physiology of the Rubber Tree Latex, CRC Press, Boca Raton, Florida, 1989.
[2] T.D. Pendle, P.E. Swinyard, The particle size of natural rubber latex concentrates by photon correlation spectroscopy, J. Nat. Rubber Res. 6 (1991) 1–11.
[3] J.B. Gomez, S. Hamzah, Particle size distribution in *Hevea* latex — some observations on the electron microscopic method, J. Nat. Rubber Res. 4 (1989) 204–211.
[4] D.F. Wood, K. Cornish, Microstructure of purified rubber particles, Int. J. Plant Sci. 161 (2000) 435–445.
[5] N. Ohya, Y. Tanaka, R. Wititsuwannakul, T. Koyama, Activity of rubber transferase and rubber particle size in *Hevea* latex, J. Rubber Res. 3 (2000) 214–221.
[6] A.P. Singh, S.G. Wi, G.C. Chung, Y.S. Kim, H. Kang, The micromorphology and protein characterization of rubber particles in *Ficus carica*, *Ficus benghalensis* and *Hevea brasiliensis*, J. Exp. Bot. 54 (2003) 985–992.
[7] J. Sansatsadeekul, J. Sakdapipanich, P. Rojruthai, Characterization of associated proteins and phospholipids in natural rubber latex, J. Biosci. Bioeng. 111 (2011) 628–634.

[8] C.C. Ho, W.L. Ng, Surface study on the rubber particles in pretreated *Hevea* latex system, Colloid Polym. Sci. 257 (1979) 406–412.
[9] W.G. Wren, Application of the Langmuir trough to the study of rubber latex, Trans. Rubber Ind. 10 (1941) 355–364.
[10] K. Nawamawat, J.T. Sakdapipanich, C.C. Ho, Y. Ma, J. Song, J.G. Vancso, Surface nanostructure of *Hevea brasiliensis* natural rubber latex particles, Colloid Surface A 390 (2011) 157–166.
[11] D.J. Siler, M. Goodrich-Tanrikulu, K. Cornish, A.E. Stafford, T.A. McKeon, Composition of rubber particles of *Hevea brasiliensis*, *Parthenium argentatum*, *Ficus elastica*, *and Euphorbia lactiflua* indicates unconventional surface structure, Plant Physiol. Biochem. 35 (1997) 881–889.
[12] K. Cornish, D.F. Wood, J.J. Windle, Rubber particles from four different species, examined by transmission electron microscopy and electron-paramagnetic-resonance spin labeling, are found to consist of a homogeneous rubber core enclosed by a contiguous monolayer biomembrane, Planta 210 (1999) 85–96.
[13] H. Hasma, A. Subramaniam, Composition of lipids in latex of *Hevea brasiliensis* clone RRIM 501, J. Nat. Rubber Res. 1 (1986) 30–40.
[14] C.C. Ho, A. Subramaniam, W.M. Yong, Lipids associated with the particles in *Hevea* latex, Proc. Int. Rubb. Conf. Kuala Lumpur, 2, 1976, pp. 441–445.
[15] S. Liengprayoon, Characterization of Lipid Composition of Sheet Rubber from *Hevea brasiliensis* and Relations with Its Structure and Properties, (PhD Thesis) Kasetsart University — Montpellier SupAgro, Kasetsart, Thailand — Montpellier, France, 2008.
[16] S. Liengprayoon, F. Bonfils, J. Sainte-Beuve, K. Sriroth, E. Dubreucq, L. Vaysse, Development of a new procedure for lipid extraction from *Hevea brasiliensis* natural rubber, Eur. J. Lipid Sci. Technol. 110 (2008) 563–569.
[17] E. Rhodes, R.O. Bishop, The lipin in hevea latex, Q. J. Rubber Res. Inst. Malaya 2 (1930).
[18] H. Hasma, Lipids associated with rubber particles and their possible role in mechanical stability of latex concentrates, J. Nat. Rubber Res. 6 (1991) 105–114.
[19] D. Blaudez, J.-M. Turlet, J. Dufourcq, D. Bard, T. Buffeteau, B. Desbat, Investigations at the air/water interface using polarization modulation IR spectroscopy, J. Chem. Soc. Faraday Trans. 92 (1996) 525–530.
[20] H. Nishimura, R.P. Philp, M. Calvin, Lipids of *Hevea brasiliensis* and *Euphorbia coerulescens*, Phytochemistry 16 (1977) 1048–1049.
[21] S. Liengprayoon, K. Sriroth, E. Dubreucq, L. Vaysse, Glycolipid composition of *Hevea brasiliensis* latex, Phytochemistry 72 (2011) 1902–1913.
[22] J. Carretero-Gonzalez, T.A. Ezquerra, S. Amnuaypornsri, S. Toki, R. Verdejo, A. Sanz, J. Sakdapipanich, B.S. Hsiao, M.A. Lopez-Manchado, Molecular dynamics of natural rubber as revealed by dielectric spectroscopy: the role of natural cross-linking, Soft Matter 6 (2010) 3636–3642.
[23] L. Tarachiwin, J. Sakdapipanich, K. Ute, T. Kitayama, T. Bamba, E. Fukusaki, A. Kobayashi, Y. Tanaka, Structural characterization of alpha-terminal group of natural rubber. 1. Decomposition of branch-points by lipase and phosphatase treatments, Biomacromolecules 6 (2005) 1851–1857.
[24] L. Tarachiwin, J. Sakdapipanich, K. Ute, T. Kitayama, Y. Tanaka, Structural characterization of alpha-terminal group of natural rubber. 2. Decomposition of branch-points by phospholipase and chemical treatments, Biomacromolecules 6 (2005) 1858–1863.
[25] L. Dai, G. Kang, Y. Li, Z. Nie, C. Duan, R. Zeng, In-depth proteome analysis of the rubber particle of *Hevea brasiliensis* (para rubber tree), Plant Mol. Biol. 82 (2013) 155–168.
[26] A. Akasawa, L.S. Hsieh, Y. Lin, Serum reactivities to latex proteins (*Hevea brasiliensis*), J. Allergy Clin. Immunol. 95 (1995) 1196–1205.
[27] A.B. Czuppon, Z. Chen, S. Rennert, T. Engelke, H.E. Meyer, M. Heber, X. Baur, The rubber elongation factor of rubber trees (*Hevea brasiliensis*) is the major allergen in latex, J. Allergy Clin. Immunol. 92 (1993) 690–697.
[28] B. Wagner, M. Krebitz, D. Buck, B. Niggemann, H.Y. Yeang, K.H. Han, O. Scheiner, H. Breiteneder, Cloning, expression, and characterization of recombinant Hev b 3, a *Hevea brasiliensis* protein associated with latex allergy in patients with *spina bifida*, J. Allergy Clin. Immunol. 104 (1999) 1084–1092.
[29] E. Sunderasan, S. Hamid, M.J. Cardosa, H.Y. Yeang, Allergenic proteins of *Hevea brasiliensis* latex fractions, J. Nat. Rubber Res. 9 (1994) 127–130.
[30] L.J. Lu, V.P. Kurup, D.R. Hoffman, K.J. Kelly, P.S. Murali, J.N. Fink, Characterization of a major latex allergen associated with hypersensitivity in *spina bifida* patients, J. Immunol. 155 (1995) 2721–2728.
[31] M.S. Dennis, D.R. Light, Rubber elongation factor from *Hevea brasiliensis*. Identification, characterization, and role in rubber biosynthesis, J. Biol. Chem. 264 (1989) 18608–18617.
[32] S.K. Oh, H. Kang, D.H. Shin, J. Yang, K.S. Chow, H.Y. Yeang, B. Wagner, H. Breiteneder, K.H. Han, Isolation, characterization, and functional analysis of a novel cDNA clone encoding a small rubber particle protein from *Hevea brasiliensis*, J. Biol. Chem. 274 (1999) 17132–17138.
[33] R. Wititsuwannakul, K. Rukseree, K. Kanokwiroon, D. Wititsuwannakul, A rubber particle protein specific for *Hevea* latex lectin binding involved in latex coagulation, Phytochemistry 69 (2008) 1111–1118.
[34] I.J. Kim, S.B. Ryu, Y.S. Kwak, H. Kang, A novel cDNA from *Parthenium argentatum* Gray enhances the rubber biosynthetic activity *in vitro*, J. Exp. Bot. 55 (2004) 377–385.
[35] A. Hillebrand, J.J. Post, D. Wurbs, D. Wahler, M. Lenders, V. Krzyzanek, D. Prüfer, C.S. Gronover, Down-Regulation of small rubber particle protein expression affects integrity of rubber particles and rubber content in *Taraxacum brevicorniculatum*, PLoS One 7 (2012) e41874.
[36] H.Y. Yeang, K.F. Cheong, E. Sunderasan, S. Hamzah, N.P. Chew, S. Hamid, R.G. Hamilton, M.J. Cardosa, The 14.6 kd rubber elongation factor (Hev b 1) and 24 kd (Hev b 3) rubber particle proteins are recognized by IgE from patients with *spina bifida* and latex allergy, J. Allergy Clin. Immunol. 98 (1996) 628–639.
[37] A.R. Bahri, S. Hamzah, Immunocytochemical localization of rubber membrane protein in *Hevea* latex, J. Nat. Rubber Res. 11 (1996) 88–95.
[38] B.L. Archer, B.G. Audley, E.G. Cockbain, G.P. McSweeney, The biosynthesis of rubber. Incorporation of mevalonate and isopentenyl pyrophosphate into rubber by *Hevea brasiliensis* latex fractions, Biochem. J. 89 (1963) 565–574.
[39] P. Rojruthai, J.T. Sakdapipanich, S. Takahashi, L. Hyegin, M. Noike, T. Koyama, Y. Tanaka, *In vitro* synthesis of high molecular weight rubber by *Hevea* small rubber particles, J. Biosci. Bioeng. 109 (2010) 107–114.
[40] L. Tarachiwin, J. Sakdapipanich, Y. Tanaka, Relationship between particle size and molecular weight of rubber from *Hevea brasiliensis*, Rubber Chem. Technol. 78 (2005) 694–704.
[41] K. Berthelot, S. Lecomte, Y. Estevez, B. Coulary-Salin, A. Bentaleb, C. Cullin, A. Deffieux, F. Peruch, Rubber elongation factor (REF), a major allergen component in *Hevea brasiliensis* latex has amyloid properties, PLoS One 7 (2012) e48065.
[42] K. Cornish, R.A. Backhaus, Rubber transferase activity in rubber particles of guayule, Phytochemistry 29 (1990) 3809–3813.
[43] J. Couthouis, K. Rebora, F. Immel, K. Berthelot, M. Castroviejo, C. Cullin, Screening for toxic amyloid in yeast exemplifies the role of alternative pathway responsible for cytotoxicity, PLoS One 4 (2009) e4539.
[44] H.P. Ta, K. Berthelot, B. Coulary-Salin, B. Desbat, J. Géan, L. Servant, C. Cullin, S. Lecomte, Comparative studies of nontoxic and toxic amyloids interacting with membrane models at the air–water interface, Langmuir 27 (2011) 4797–4807.
[45] G. Rouser, S. Fleischer, A. Yamamoto, Two dimensional thin layer chromatographic separation of polar lipids and determination of phospholipids by phosphorus analysis of spots, Lipids 5 (1970) 494–496.
[46] E.J. Dufourc, Solid state NMR in biomembranes, in: B. Larijani, R. Woscholski, C.A. Rosser (Eds.), Chemical Biology, Wiley J & Sons, Ltd, London, 2006, pp. 113–131.
[47] A. Grelard, C. Loudet, A. Diller, E.J. Dufourc, NMR Spectroscopy of Lipid Bilayers, vol. 654, Humana Press Inc, Totowa, 2006.
[48] E. Goormaghtigh, V. Raussens, J.-M. Ruysschaert, Attenuated total reflection infrared spectroscopy of proteins and lipids in biological membranes, Biochim. Biophys. Acta Biomembr. 1422 (1999) 105–185.
[49] S. Castano, B. Desbat, Structure and orientation study of fusion peptide FP23 of gp41 from HIV-1 alone or inserted into various lipid membrane models (mono-, bi- and multibi-layers) by FT-IR spectroscopies and Brewster angle microscopy, Biochim. Biophys. Acta Biomembr. 1715 (2005) 81–95.
[50] J.H. Davis, K.R. Jeffrey, M. Bloom, M.I. Valic, T.P. Higgs, Quadrupolar echo deuteron magnetic resonance spectroscopy in ordered hydrocarbon chains, Chem. Phys. Lett. 42 (1976) 390–394.
[51] M. Rance, R. Byrd, Obtaining high-fidelity spinning 1/2 powder spectra in anisotropic media: phase cycled Hahn echo spectroscopy, J. Magn. Reson. 52 (1983) 221–240.
[52] Z. Salamon, G. Tollin, I. Alves, V. Hruby, Chapter 6 plasmon resonance methods in membrane protein biology: applications to GPCR signaling, in: M.H. Tracy, J.H. Damon (Eds.), Method Enzymol., vol. 461, Academic Press, 2009, pp. 123–146.
[53] P. Mueller, D.O. Rudin, H. Ti Tien, W.C. Wescott, Reconstitution of cell membrane structure *in vitro* and its transformation into an excitable system, Nature 194 (1962) 979–980.
[54] U. Sookmark, V. Pujade-Renaud, H. Chrestin, R. Lacote, C. Naiyanetr, M. Seguin, P. Romruensukharom, J. Narangajavana, Characterization of polypeptides accumulated in the latex cytosol of rubber trees affected by the tapping panel dryness syndrome, Plant Cell Physiol. 43 (2002) 1323–1333.
[55] F. Aussenac, M. Laguerre, J.M. Schmitter, E.J. Dufourc, Detailed structure and dynamics of bicelle phospholipids using selectively deuterated and perdeuterated labels. H-2 NMR and molecular mechanics study, Langmuir 19 (2003) 10468–10479.
[56] B. Larijani, D.L. Poccia, L.C. Dickinson, Phospholipid identification and quantification of membrane vesicle subfractions by P-31-H-1 two-dimensional nuclear magnetic resonance, Lipids 35 (2000) 1289–1297.
[57] T. Glonek, T.O. Henderson, R.L. Hilderbrand, T.C. Myers, Biological phosphonates: determination by phosphorus-31 nuclear magnetic resonance, Science 169 (1970) 192–194.
[58] M.-L. Jobin, P. Bonnafous, H. Temsamani, F. Dole, A. Grélard, E.J. Dufourc, I.D. Alves, The enhanced membrane interaction and perturbation of a cell penetrating peptide in the presence of anionic lipids: toward an understanding of its selectivity for cancer cells, Biochim. Biophys. Acta Biomembr. 1828 (2013) 1457–1470.
[59] H.P. Ta, K. Berthelot, B. Coulary-Salin, S. Castano, B. Desbat, P. Bonnafous, O. Lambert, I. Alves, C. Cullin, S. Lecomte, A yeast toxic mutant of HET-s amyloid disrupts membrane integrity, Biochim. Biophys. Acta Biomembr. 1818 (2012) 2325–2334.
[60] G.F. Salgado, A. Vogel, R. Marquant, S.E. Feller, S. Bouaziz, I.D. Alves, The role of membranes in the organization of HIV-1 Gag p6 and Vpr: p6 shows high affinity for membrane bilayers which substantially increases the interaction between p6 and Vpr, J. Med. Chem. 52 (2009) 7157–7162.
[61] I.D. Alves, C. Bechara, A. Walrant, Y. Zaltsman, C.Y. Jiao, S. Sagan, Relationships between membrane binding, affinity and cell internalization efficacy of a cell-penetrating peptide: penetratin as a case study, PLoS One 6 (2011) e24096.
[62] I.D. Alves, Z. Salamon, V.J. Hruby, G. Tollin, Ligand modulation of lateral segregation of a G-protein-coupled receptor into lipid microdomains in sphingomyelin/phosphatidylcholine solid-supported bilayers, Biochemistry 44 (2005) 9168–9178.
[63] K. Berthelot, C. Cullin, S. Lecomte, What does make an amyloid toxic: morphology, structure or interaction with membrane? Biochimie 95 (2013) 12–19.
[64] E.J. Dufourc, S. Buchoux, J. Toupe, M.A. Sani, F. Jean-Francois, L. Khemtemourian, A. Grelard, C. Loudet-Courreges, M. Laguerre, J. Elezgaray, B. Desbat, B. Odaert, Membrane interacting peptides: from killers to helpers, Curr. Protein Pept. Sci. 13 (2012) 620–631.

[65] S. Buchoux, J. Lai-Kee-Him, M. Garnier, P. Tsan, F. Besson, A. Brisson, E.J. Dufourc, Surfactin-triggered small vesicle formation of negatively charged membranes: a novel membrane-lysis mechanism, Biophys. J. 95 (2008) 3840–3849.
[66] Q. Xiang, K. Xia, L. Dai, G. Kang, Y. Li, Z. Nie, C. Duan, R. Zeng, Proteome analysis of the large and the small rubber particles of *Hevea brasiliensis* using 2D-DIGE, Plant Physiol. Biochem. 60 (2012) 207–213.
[67] A. Villar-Pique, R. Sabate, O. Lopera, J. Gibert, J.M. Torne, M. Santos, S. Ventura, Amyloid-like protein inclusions in tobacco transgenic plants, PLoS One 5 (2010) e13625.
[68] H. Mira, M. Vilar, V. Esteve, M. Martinell, M. Kogan, E. Giralt, D. Salom, I. Mingarro, L. Penarrubia, E. Perez-Paya, Ionic self-complementarity induces amyloid-like fibril formation in an isolated domain of a plant copper metallochaperone protein, BMC Struct. Biol. 4 (2004) 7.
[69] T. Konno, K. Murata, K. Nagayama, Amyloid-like aggregates of a plant protein: a case of a sweet-tasting protein, monellin, FEBS Lett. 454 (1999) 122–126.
[70] B.G. Audley, The isolation and composition of helical protein microfibrils from *Hevea brasiliensis* latex, Biochem. J. 98 (1966) 335–341.
[71] B.L. Kagan, H. Jang, R. Capone, F. Teran Arce, S. Ramachandran, R. Lal, R. Nussinov, Antimicrobial properties of amyloid peptides, Mol. Pharm. 9 (2011) 708–717.

SUPPLEMENTARY MATERIALS

Rubber particle proteins, HbREF and HbSRPP, show different interactions with model membranes

Karine Berthelot[1*], Sophie Lecomte[2], Yannick Estevez[1], Vanessa Zhendre[3], Sarah Henry[2,4], Julie Thévenot[1], Erick J. Dufourc[2,3], Isabel D. Alves[2] and Frédéric Peruch[1*]

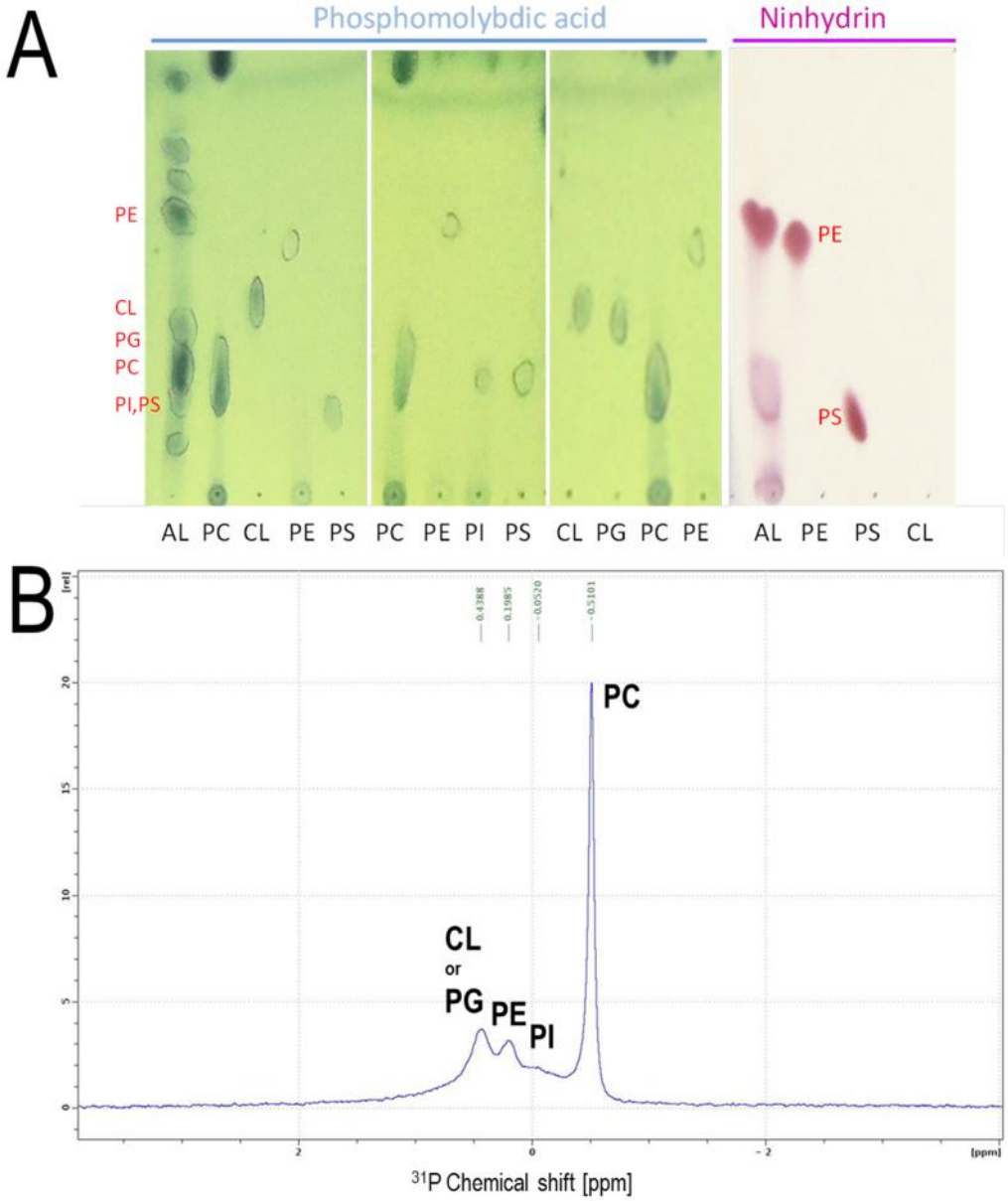

Supplementary Fig. S1. Composition of asolectin (Sigma #11145). A) Thin layer chromatographies (Silica Gel60 F_{254}, Merck) were developped in $CHCL_3/MeOH/H_2O$ (65:25:4 v/v) as described in Ho *et al.*, 1976. (*Proc. Int. Rubb. Conf. Kuala Lumpur* 2, 441-445). Phospholipids were stained with phosphomolybdic acid (Sigma; 10 % solution) and amines with ninhydrin (Sigma; 0.5 % in butanol-1). B) ^{31}P liquid-NMR of asolectin in $CDCL_3/MD_3OD$ (80:20 v/v). Assignment is made on the basis of litterature data and using ^{1}H-^{31}P 2D-NMR spectroscopy. Abbreviations: asolectin, AL; phosphatidyl choline, PC; cardiolipin, CL; phosphatidyl ethanolamine, PE; phosphatidyl serine, PS; phosphatidyl inositol, PI; phosphatidyl glycerol, PG.

Supplementary Figure S1
Berthelot *et al.*, 2013

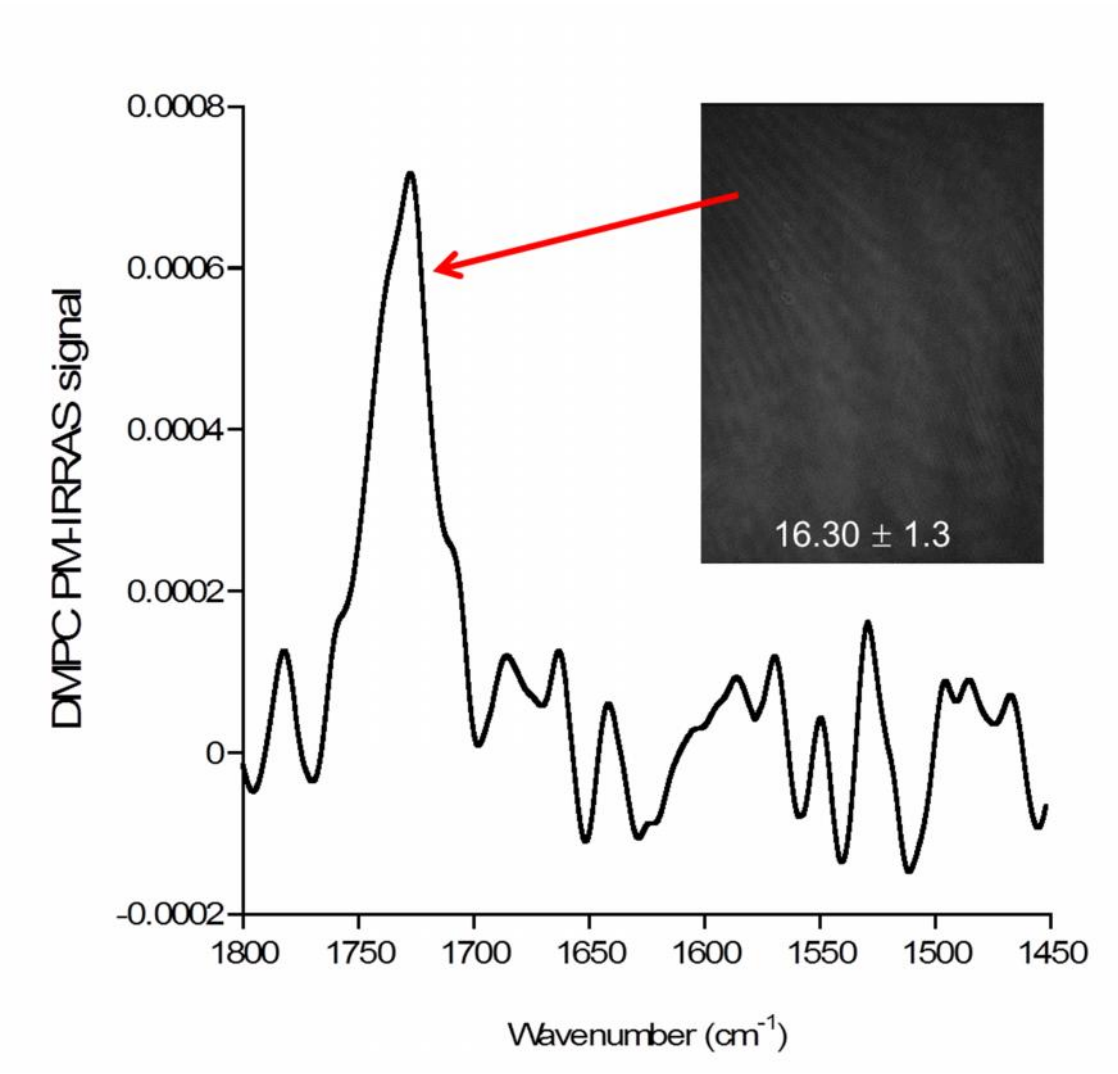

Supplementary Fig. S2. PM-IRRAS spectrum of a DMPC monolayer with corresponding ellipsometric image and thickness.

Supplementary Figure S2
Berthelot *et al.*, 2013

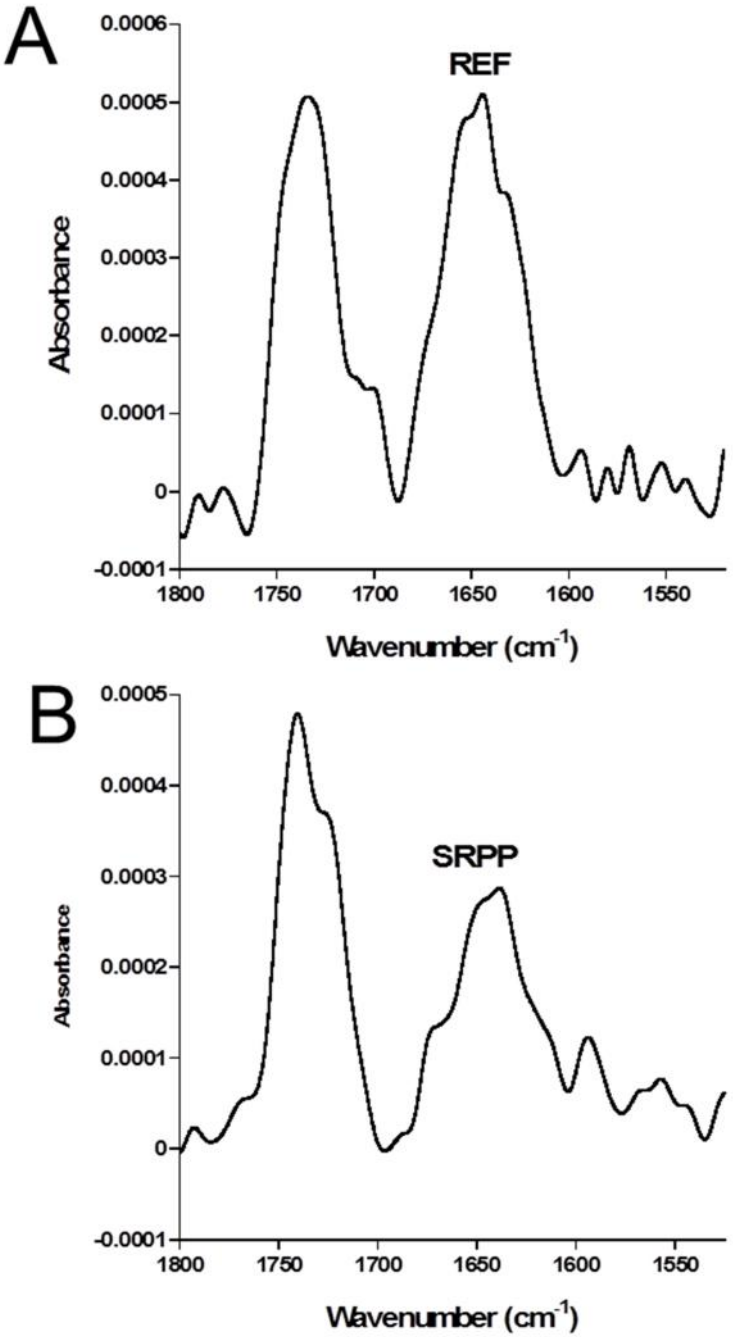

Supplementary Fig. S3. REF and SRPP structures in interaction with an egg PC bilayer from fusionned SUVs by ATR-FTIR. Spectra of the SUV bilayer with REF (A) and with SRPP (B). Region 1800-1600 cm-1 is corresponding to the phospholipid C-O band (left) and amide I band (CO-NH) of the protein. For the experiment, egg PC SUVs were spread on the ATR crystal to form a regular bilayer, and then carefully washed with D_2O. Proteins were incubated at 50 µM on the top of the bilayer for 10 min and then washed 3 times before recording spectra.

Supplementary Figure S3
Berthelot *et al.,* 2013

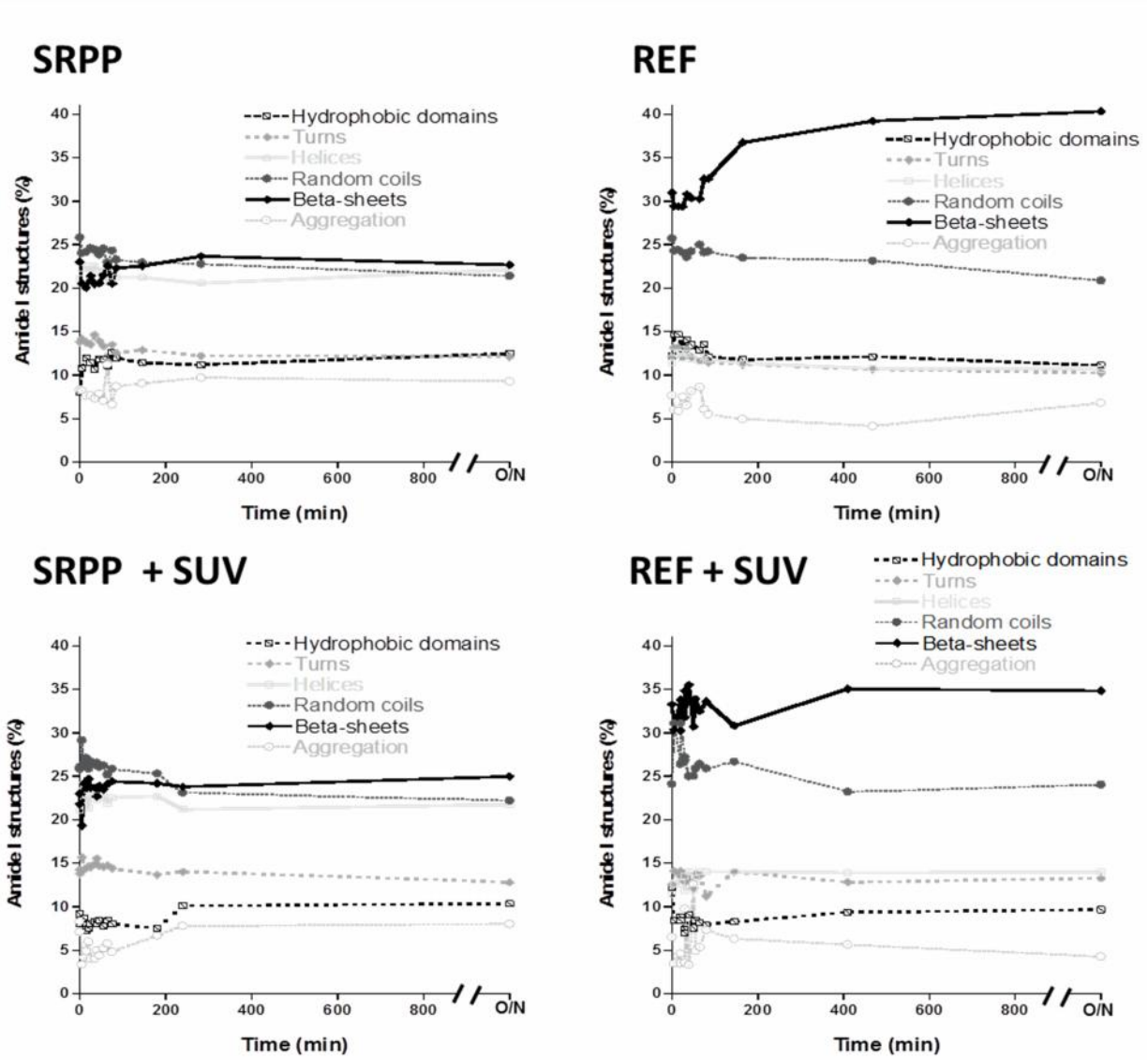

Supplementary Fig. S4. Kinetics of structuration of REF and SRPP in absence or in presence of DMPC SUVs. Kinetics was followed by ATR-FTIR and results are presented as the relative % of amide structures after spectra deconvolution. SRPP does not show major changes over times and its structure does not vary in presence of SUVs. REF rapidly aggregated and structured in β-sheets in a time dependent manner and its amyloid polymerization may be inhibited by the presence of lipids. Incubations were performed in PBS, at 50 µM and 37°C. DMPC SUVs were added at *Ri=50*.

Supplementary Figure S4
Berthelot *et al.*, 2013

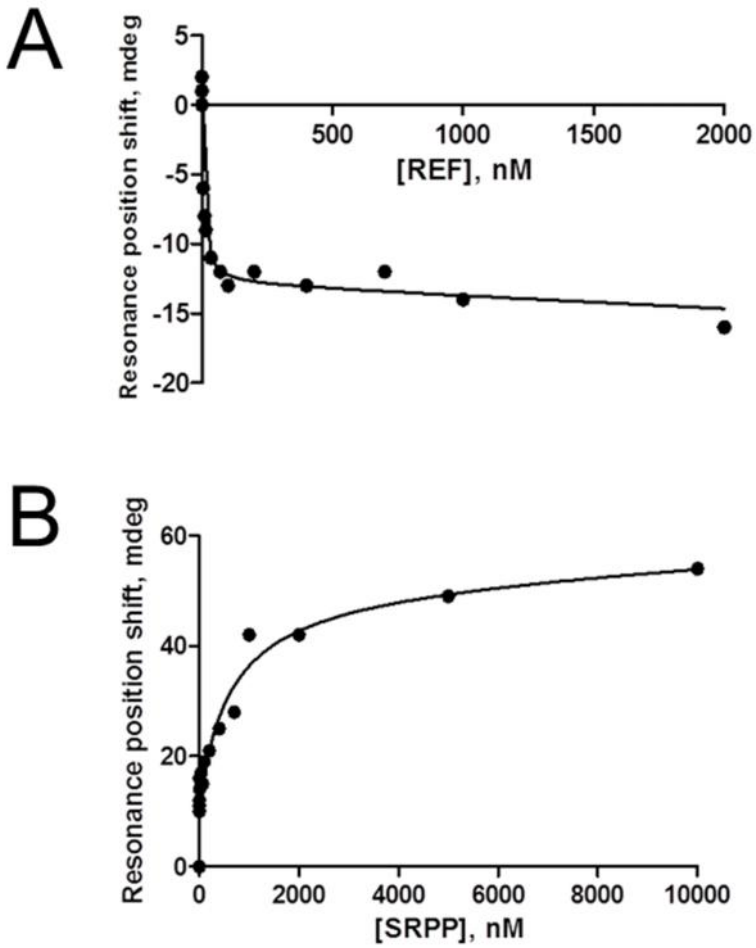

Supplementary Fig. S5. Evaluation of REF and SRPP affinity towards egg PC bilayer by PWR. Hyperbolic fits of the resonance minimum position shifts as a function of concentration are given using *p*-polarization data for REF (A) and *s*-polarization data for SRPP (B). REF and SRPP proteins were injected into the cell sample compartment containing the cell membrane in an incremental fashion from 100 pM to 10 µM at 25°C. Only an estimative value of the apparent affinity constant for the two proteins to the membrane may be produced and indicates that REF has an apparent affinity to the membrane in the low nanomolar order, about 100 times higher than SRPP.

Supplementary Figure S5
Berthelot *et al.*, 2013

SUPPLEMENTARY TABLE S1

Sequences, homology and physico-chemical parameters of His-tagged REF and SRPP

Sequences:

```
REF     :MAEDEDNQQGQGEGLKYLGFVQDAATYAVTTFSNVYLFAKDKSGPLQPGVDIIEGPVKNVAVPLYNRFSYIPNGALKFVD :80
SRPP    :MAEEVE-----EERLKYLDFVRAAGVYAVDSFSTLYLYAKDISGPLKPGVDTIENVVKTVVTPVY----YIPLEAVKFVD :71

REF     :STVVASVTIIDRSLPPIVKDASIQVVSAIRAAPEAARSLAS-SLPGQTKILAKVFYGEN--------------------:138
SRPP    :KTVDVSVTSLDGVVPPVIKQVSAQTYSVAQDAPRIVLDVASSVFNTGVQEGAKALYANLEPKAEQYAVITWRALNKLPLV:151

REF     :------------------------------------------------------------------------------ :138
SRPP    :PXLEPKAEQYAVITWRALNKLPLVPQVANVVVPTAVYFSEKYNDVVRGTTEQGYRVSSYLPLLPTEKITKVFGDEAS :204
```

Proteins	Amino Acids	MW (kDa)	pI	Ext. Coefficient ($L.mol^{-1}.cm^{-1}$)	Net charge	Hydropathicity
REF	147	15.8	6.3	8940	-2	-0.084
SRPP	213	23.4	5.5	24870	-6	0.003

Data at pH 7.4, and grand average of hydropathicity (GRAVY) were estimated from the amino-acid sequence of each protein fused to the N-terminal His tag (sequence MHHHHHHGS). Data were obtained from ExPASy proteomics Server, http://expasy.org/tools/protparam.html.